Synthesis, physical properties, and chemistry of donor/acceptor substituted pentacenes

Dan Lehnherr,[a] Matthias Adam,[b] Adrian H. Murray,[a] Robert McDonald,[c] Frank Hampel,[b] and Rik R. Tykwinski*[a,b †]

[a] Department of Chemistry, University of Alberta, Edmonton, Alberta, T6G 2G2, Canada.

[b] *Department of Chemistry and Pharmacy & Interdisciplinary Center for Molecular Materials (ICMM), Friedrich-Alexander-Universität, Erlangen-Nürnberg, Henkestr. 42, 91054 Erlangen, Germany, Fax: +49-913-185-26865; Tel: +49-913-185-22540,E-mail: rik.tykwinski@fau.de*

[c] *X-ray Crystallography Lab, Department of Chemistry, University of Alberta, Edmonton, Alberta, T6G 2G2, Canada*

† Dedicated to Professor Reginald (Reg) Mitchell, with thanks for his support and collegiality through the years – thanks Reg!

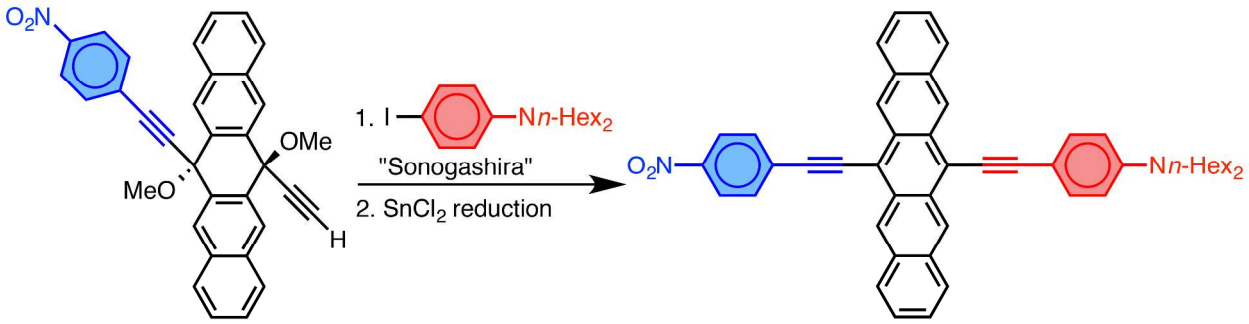

Abstract. Pentacenes bearing electron donating and/or withdrawing groups, namely methoxy, dialkylamino-, and nitroaryl moieties, are synthesized to afford polarized pentacenes. The optical, electrochemical, and chemical properties of these derivatives are explored. The cycloaddition reaction of selective derivatives with tetracyanoethylene (TCNE) is explored, and the experimental results are rationalized on the basis calculations using density functional theory (DFT). X-ray crystallographic data provides insight molecular structure and intermolecular interactions present in the solid-state.

Keywords. pentacene • donor-acceptor • acene • polycyclic aromatic hydrocarbon • TCNE cycloaddition • density functional theory

Introduction. Structural variation is used to modify HOMO–LUMO energies, band gaps, solid-state packing, and numerous other structure-related properties in optoelectronic chromophores.[1,2,3,4] To this end, the stepwise assembly of pentacenes has afforded structures with unusual and potentially useful structures.[5,6,7,8] The functionalization of pentacene is typically achieved via two general approaches, placement of desired groups at the pro-cata positions (particularly the 2,3,9,10-positions, blue spheres in Figure 1) or at the peri-positions (particularly the 6,13-positions, red spheres in Figure 1). For example, pro-cata functionalization can be achieved with alkoxy,[9] alkyl,[10] alkynyl,[11] aryl,[12] carboxyl,[10a–b,13] silyl,[14] halo,[15] and cyano[16] groups. Functionalization of the 6,13-positions have been realized with alkyl,[17] silylethynyl,[18] aryl,[19] arylethynyl,[20] thioalkyl,[21] cyano,[22] trifluoromethyl,[23] and Pt-acetylide[24] groups, commonly via a 6,13-pentacenequinone precursor. The fusion of quinone,[25] imide,[26] or arene[27] moieties to pentacene or the incorporation of heteroatoms into the chromophore can also be accomplished.[28] These various substituents and substitution patterns can affect a wide range of properties including HOMO-LUMO energies, optical absorption/emission properties, solid-state packing, charge transport characteristics, and photostability.[1,2,19b,29]

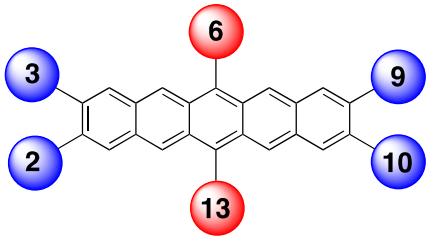

Figure 1. Summary of common pentacene functionalization patterns: (a) Blue spheres illustrate the 2,3,9,10-positions (pro-cata positions) and (b) red spheres illustrate the 6,13-positions (peri-positions).

The formation of pentacenes with unsymmetrical 6,13-substitution can provide polarized

pentacenes with weak donor and acceptor substituents (e.g., **1d,e** Scheme 1).[30, 31] Unfortunately, the synthetic protocol used in these cases, nucleophilic addition to pentacene quinone, does not tolerate strong electron-donating or -withdrawing groups such as the aniline and nitrophenyl moieties.[30, 32] This problem has now been solved through derivatization of the protected precursors **2a** and **2b** via palladium catalyzed Sonogashira cross-coupling reactions with aryl iodides. It should be emphasized that intermediates **2a,b** and related structures provide powerful building blocks for a wide range of cross-coupling,[7,33] cycloaddition,[34] and coordination[35] reactions as recently demonstrated in the synthesis of oligomeric pentacenes and inorganic complexes with functionalized pentacenes.

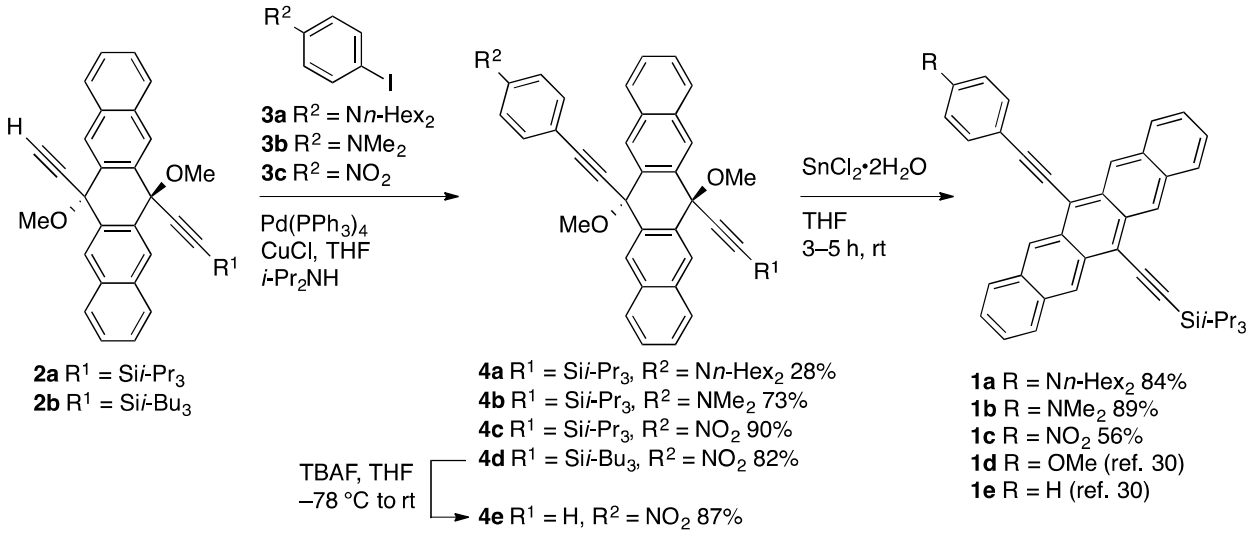

Scheme 1. Synthesis of **4a–e** and **1a–c** (this work) and structures of **1d,e** (from ref. 30).

Synthesis of donor/acceptor pentacenes. The reaction of **2a,b**[7] with iodoaryl derivatives **3a–c** afforded **4a–d**. Aniline derivative **4a** partially decomposed during chromatographic purification on silica gel, leading to a low isolated yield. Dimethylaniline substituted **4b** was likewise unstable on silica gel, but could be isolated pure and in high yield via recrystallization (see SI for details). Nitrobenzene derivative **4c** was, on the other hand,

stable to purification via column chromatography. Sn^{II}-mediated reductive aromatization of **4a–c** provided **1a–c** (a shorter reaction time was used for the synthesis of **1c** to minimize the reduction of the nitro group).[36]

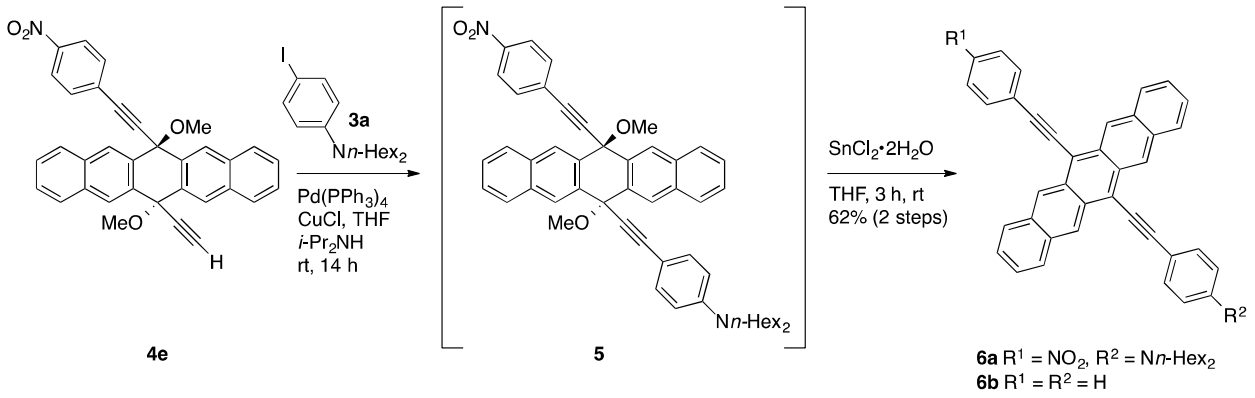

Scheme 2. Synthesis of donor-acceptor pentacene **6a** and structure of diphenyl derivative **6b** (see SI for the synthesis of **6b**).

A push-pull pentacene was then targeted. This began with the conversion of **4d** to **4e** via reaction with TBAF at low temperature to avoid products resulting from fluorodenitration (Scheme 1).[37] A Sonogashira reaction of **4e** with **3a** then installed the dialkylaniline group, affording **5** (Scheme 2). Compound **5** was also unstable to purification on silica gel. Thus, after aqueous workup, the crude product was aromatized without prior chromatographic purification to provide donor-acceptor pentacene **6a**, which could be isolated pure in 62% yield via column chromatography and crystallization.

Characterization of donor/acceptor pentacenes. UV–vis spectroscopy in CH_2Cl_2 reveals λ_{max} is moderately influenced by substitution changes in compounds **1a–e** and **6a** (Figures 2 and 3).[38] Parent compound **1e** (R = H) has λ_{max} = 652 nm, and this absorption is red-shifted via incorporation of increasingly electron donating groups to 655 nm (**1d**, R = OMe), 668 nm (**1b**, R = NMe_2), and 674 nm (**1a**, R = N*n*-Hex_2). Appending a nitroaryl group gives λ_{max} = 666 nm for **1c**, nearly equal to that of donor substituted **1b**. The most strongly polarized pentacene derivative

6a (density functional calculations predict a dipole moment of 13.7 Debye, see SI for details) shows the lowest energy λ_{max} at 689 nm, noticeably red-shifted versus the parent chromophore **6b**[20a,39] (λ_{max} 660 nm) as well as derivatives **1a–d**. The red-shift for **6a** is most dramatic in the solid state (see Figure S5), where the UV–vis spectrum of a thin film shows λ_{max} = 823 nm, shifted by 134 nm to lower energy than that in solution. Donor/acceptor pentacenes **1a–c** and **6a** show no significant emission in CH_2Cl_2.

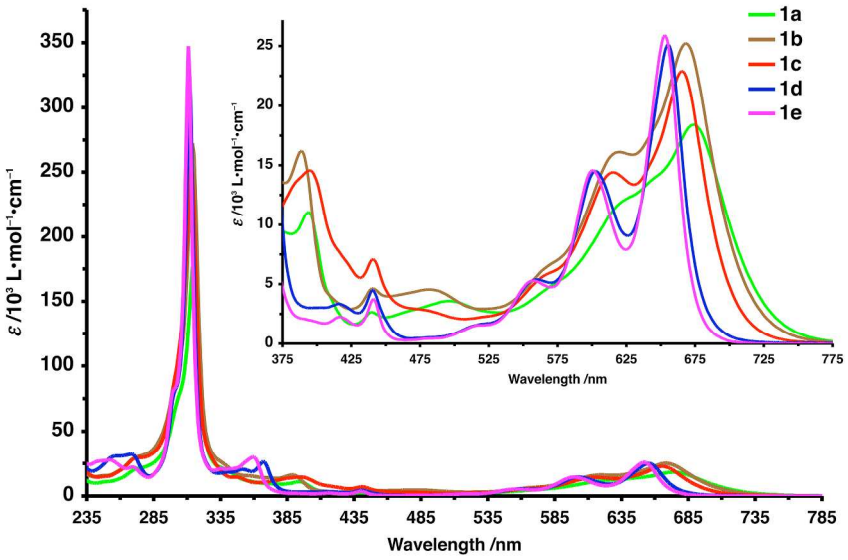

Figure 2. UV-vis absorption spectra of **1a–e** in CH_2Cl_2; inset expansion of low-energy region of UV-vis absorption spectra.

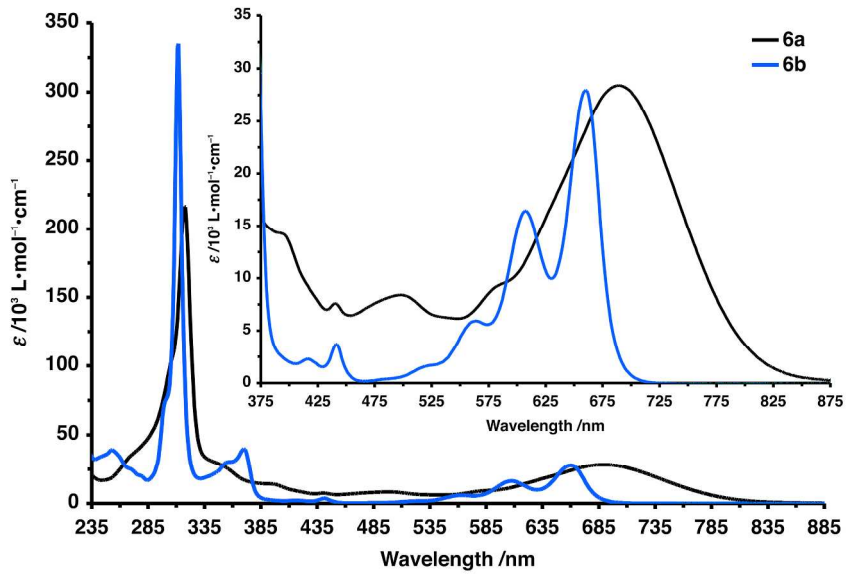

Figure 3. UV-vis absorption spectra of **6a,b** in CH_2Cl_2; inset expansion of low-energy region of UV-vis absorption spectra.

Table 1. Optoelectronic, electrochemical, and thermal properties of pentacenes **1a–e** and **6a,b**.

Cmpd	λ_{max} (CH_2Cl_2) /nm [a]	λ_{max} (film) /nm [b]	Red Shift /nm [c]	E_g^{opt} (CH_2Cl_2) /eV [d]	$E_g^{electro}$ /eV [e]	E_{ox1} /V [e]	E_{ox2} /V [e]	E_{red1} /V [e]	E_{red2} /V [e]	E_{red3} /V [e]
1a	674	685	11	1.66	1.63	0.16 [f]	0.41 [f]	–1.47	–1.94	
1b	668	683	15	1.68	1.66	0.18 [f]	0.43 [f]	–1.48	–1.93 [f]	
1c	666	718	52	1.72	1.77	0.44		–1.33	–1.46	–2.09
1d	655	668	13	1.78	1.80	0.35		–1.45	–1.92	
1e	652	671	19	1.81	1.83	0.39		–1.44	–1.90	
6a	689	823	134	1.49	1.52	0.18	0.39 [f]	–1.34	–1.48	–2.08 [f]
6b	660	– [g]	– [g]	1.78	1.75	0.33		–1.42	–1.84	

[a] Lowest energy absorption maximum. [b] Thin film drop cast from CH_2Cl_2. [c] Red-shift for the longest wavelength absorption λ_{max} measured between the solid and solution states. [d] As determined from UV–vis spectroscopy, see reference 40. [e] Cyclic voltammetry performed in benzene/MeCN (3:1 v/v) with 0.1 M *n*-Bu_4NPF_6 as supporting electrolyte at a scan rate of 150

mV/s. Potentials are referenced to the ferrocene/ferrocenium (Fc/Fc^+) couple used as an internal standard.[41] [f] Quasi-reversible event. [g] Data not measured.

Cyclic voltammetry (CV) has been used as a complementary method to UV–vis spectroscopy to examine the electronic make up of donor/acceptor pentacenes (Table 1).[41] The presence of the electron-donating aniline groups significantly raises the energy of the HOMO, as observed by lower oxidation potentials for **1a** and **1b** (E_{ox} = 0.16 and 0.18 V, respectively) relative to parent compound **1e** (E_{ox} = 0.39 V). Reduction of nitro derivative **1c**, on the other hand, is observed at a lower potential (–1.33 V) than **1e** (E_{red} –1.44 V) and correlating with a lower LUMO level. For donor-acceptor **6a**, E_{ox1} = 0.18 V is nearly identical to **1a** and **1b**, while E_{red1} = –1.34 V is analogous to that of **1c**, showing that the aniline and nitro groups dictate the initial redox events of **6a**.

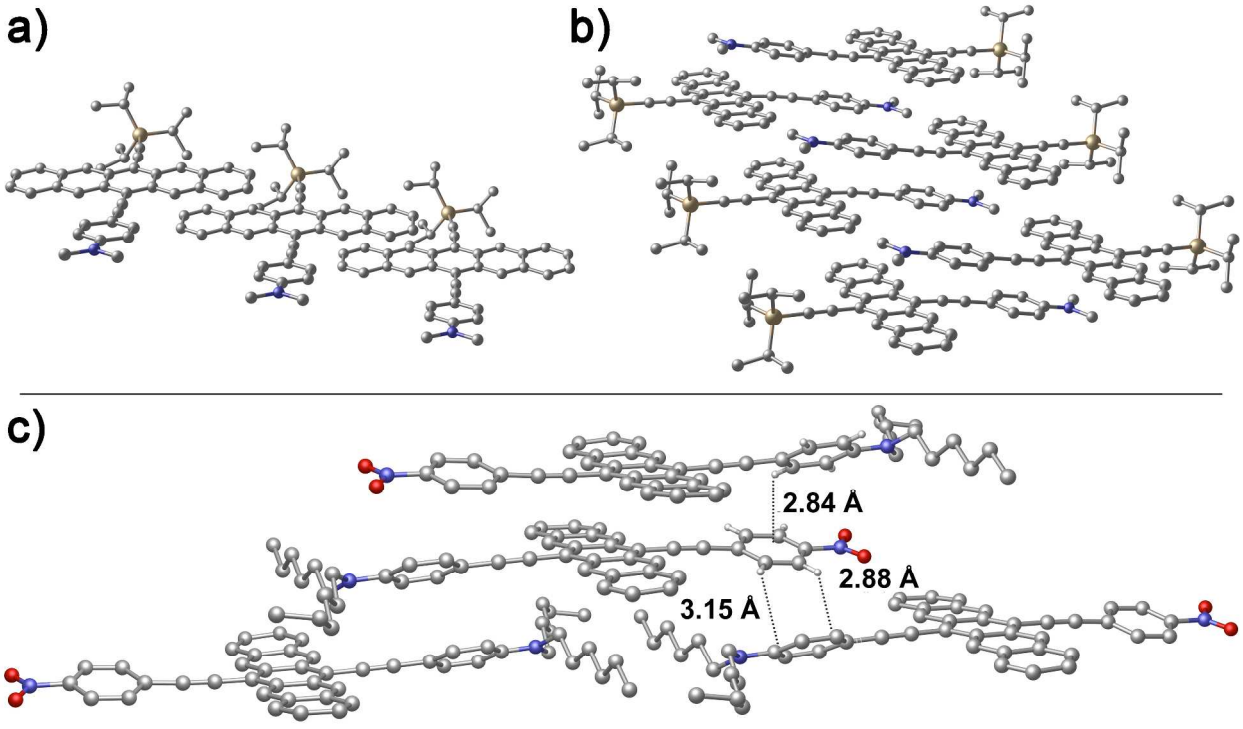

Figure 4. Solid-state packing of (a) pentacene **1b** viewed down the short molecular axis, (b) pentacene **1b** viewed down the long molecular axis, and (c) pentacene **6a** viewed down the long

molecular axis showing three C–H•••π interactions. Solvent molecules and hydrogen atoms omitted in (a–b); carbon = gray, nitrogen = purple, oxygen = red, silicon = gold.

Trends for electrochemical HOMO–LUMO gap ($E_g^{electro}$) are reasonably consistent with that calculated from the UV–vis data (E_g^{opt}) for **1a–e** and **6a,b**[40] varying only by ±0.05 eV. Comparing $E_g^{electro}$ values, those of **1d–e** are the highest 1.80–1.83 eV, while a slightly lower value $E_g^{electro}$ = 1.77 eV is found for nitro derivative **1c**. Aniline derivatives **1a,b** show a further lowering of $E_{\mathrm{g}}^{\mathrm{electro}}$ (1.63 eV and 1.66 eV, respectively), and the greatest effect is observed for donor-acceptor **6a** with $E_g^{electro}$ = 1.52 eV (E_g^{opt} of 1.49 eV), confirming the ability to influence HOMO and LUMO levels through substitution.

X-ray crystallographic structures of compound **1b** and **6a** are shown in Figure 4. The packing of **1b**•0.5CH_2Cl_2 shows a 1-D slipped π-stacking arrangement with about two benzene rings worth of overlap and an interplanar distance between pentacene moieties of 3.40 Å.[42] The solid-state packing of **6a** features centrosymmetric cofacial dimeric pairs with interplanar distance between pentacenes of 3.46 Å.[42] Although no long-range cofacial π-stacking is present, a number of C–H•••π interactions[43] seem to guide the long-range arrangement of **6a**. The C–H bonds from the electron deficient nitroaryl moiety point into the faces of the adjacent electron rich aniline rings, which are likely the cause of the non-planar arrangement of the pendent aryl rings with respect to the pentacene framework. Furthermore, the hexyl chains from the aniline group appear to engage in C–H•••π interactions with the aromatic core of the pentacene, with distances that range from 2.82 to 3.20 Å (see Figure S2). The nitroaryl group and the pentacene moiety show a 14.6° dihedral angle, while the dihedral angle between the aniline and the pentacene moieties is –27.6° (in the opposite direction).

Reactions with TCNE. Oligoacenes are known to undergo cycloaddition chemistry with a variety of cycloaddition partners including molecular oxygen, acetylene derivatives, arynes, fullerenes, as well as dimerization processes via [4+4] and others. [44] The cycloaddition/cycloreversion of tetracyanoethylene (TCNE) with electron rich alkynes is a simple and mild reaction for the formation of optoelectronic materials with interesting properties.[45] With the intent to form pentacene derivatives with an even stronger acceptor group, the reaction of TCNE with **1b** was attempted toward the synthesis of **7b** (Scheme 3).[46] This reaction resulted in a mixture of products, from which the isolation of **7b** was unsuccessful. The analogous reaction using **1d**, on the other hand, gave the Diels-Alder adduct **8d**, as confirmed by X-ray crystallography (Figure 5).

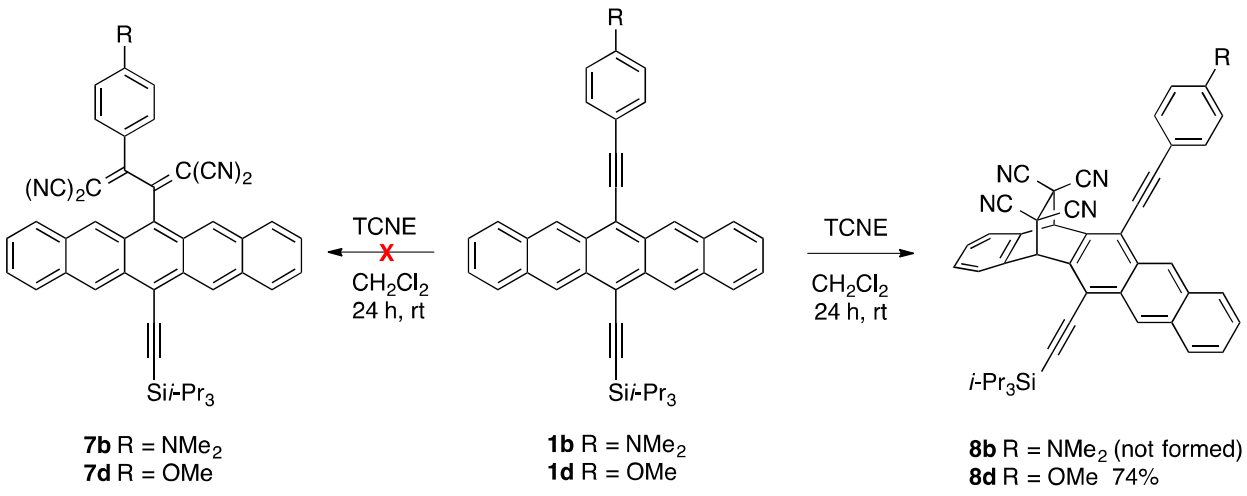

7b R = NMe_2
7d R = OMe

1b R = NMe_2
1d R = OMe

8b R = NMe_2 (not formed)
8d R = OMe 74%

Scheme 3. Structure of pentacenes **7b** and **7d** and the synthesis of adduct **8d**.

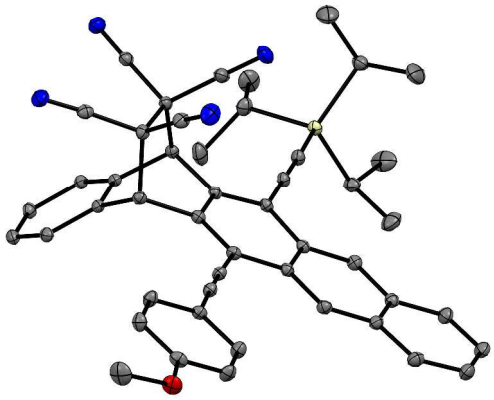

Figure 5. ORTEP representation of the X-ray crystallographic structure of **8d**. Hydrogen atom not shown, and non-hydrogen atoms are represented by Gaussian ellipsoids at the 50% probability level.

In order to gain insight into the reactivity of pentacene **1d** with TCNE and the origin for the preferential formation of the [4+2] product **7d** over the [2+2]/retro[2+2] product **8d**, we utilized density functional theory (DFT) calculations (see Figure 6, and the Supporting Information for results related to **1b**). To reduce the computational cost, the triisopropylsilyl group in **1d** (and its related structures) was replaced with a trimethylsilyl group (e.g., **1d'**). Using B3LYP/6-31G(d), DFT calculations[47] for both the [4+2] and [2+2] reactivity of **1d'** with TCNE were performed to explore: (a) whether the overall reactions to **7d'** and **8d**' are exothermic, (b) which reaction pathway leads to the thermodynamically preferred product, (c) whether there are any intermediates that are exceedingly high in energy to be reasonably accessible, and (d) whether the relative energy of key transition state structures can provide insight into the origin for the experimental preference for the [4+2] over the [2+2] pathway.

The [2+2]/retro[2+2] pathway associated with **1d'** and TCNE leads to two conformational isomers of product **7d'**, namely *s-trans*-**7d'** and *s-cis*-**7d'**, each being exothermic relative to starting materials **1d'** and TCNE by –32.0 and –31.3 kcal/mol, respectively. The formal

[2+2]-cycloaddition of TCNE with alkynes is known to proceed via stepwise mechanism[48] and our DFT results are consistent with this (Figure 6). Relative to starting materials **1d'** and TCNE, transition state **TS9d** is 31.4 kcal/mol higher in energy towards forming the first C–C bond to reach intermediate **10d** (+28.0 kcal/mol) in the stepwise formal [2+2], en route to the exothermic cyclobutene intermediate **11d** (–17.7 kcal/mol) and ultimately to products **7d'** via a retro[2+2] process. While the formal [2+2]/retro[2+2] pathway leads to the thermodynamic product, (**s-*trans*-7d'**), experimental results afford the [4+2]-product **8d**, implying a Curtin-Hammett scenario must be operational. Namely, that rate determining step leading to **7d'** along the [2+2]/retro[2+2] pathway places an energy barrier of higher energy compared to the transition state leading to the [4+2] adduct (**8d'**). Indeed the electronic energy barrier for the TCNE-acene [4+2]-cycloaddition (**TS12d** via **13d**) leading to product **8d'** is 17.8 kcal/mol lower in energy compared to the first carbon-carbon bond forming transition state (**TS9d**) in the stepwise TCNE-alkyne formal [2+2]-cycloaddition. This is the origin of the experimental preference to form product **8d** over **7d**. Analogous DFT analysis associated with dimethylamino substituted pentacene **1b** reveals a similar scenario, with preference for [4+2] over [2+2] reactivity. Although, we were not able to locate the analogous transition state **TS9b**, intermediate **10b** is significantly higher in energy (+22.3 kcal/mol relative to starting materials **1b'** and TCNE) than the [4+2] transition state (**TS12b**, +12.5 kcal/mol), thus indicating that [2+2] reactivity is also disfavoured in the case of substrate **1b** (see Supporting Information for details).

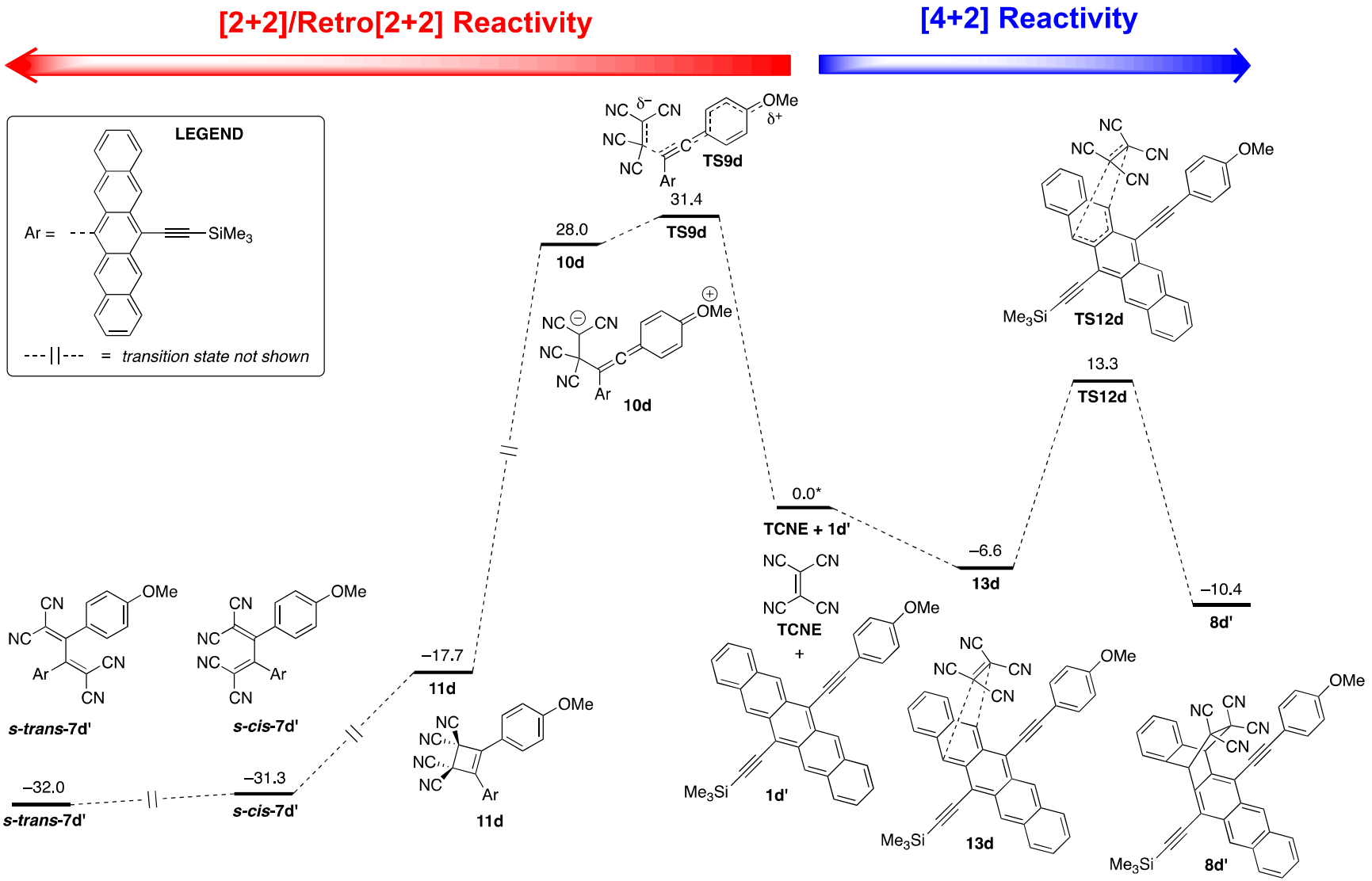

Figure 6. DFT calculated energy profile using B3LYP/6-31G(d) for reaction of TCNE with pentacene **1b** illustrating the origin of the preference for the [4+2] reactivity versus the formal [2+2]/retro[2+2] reactivity.

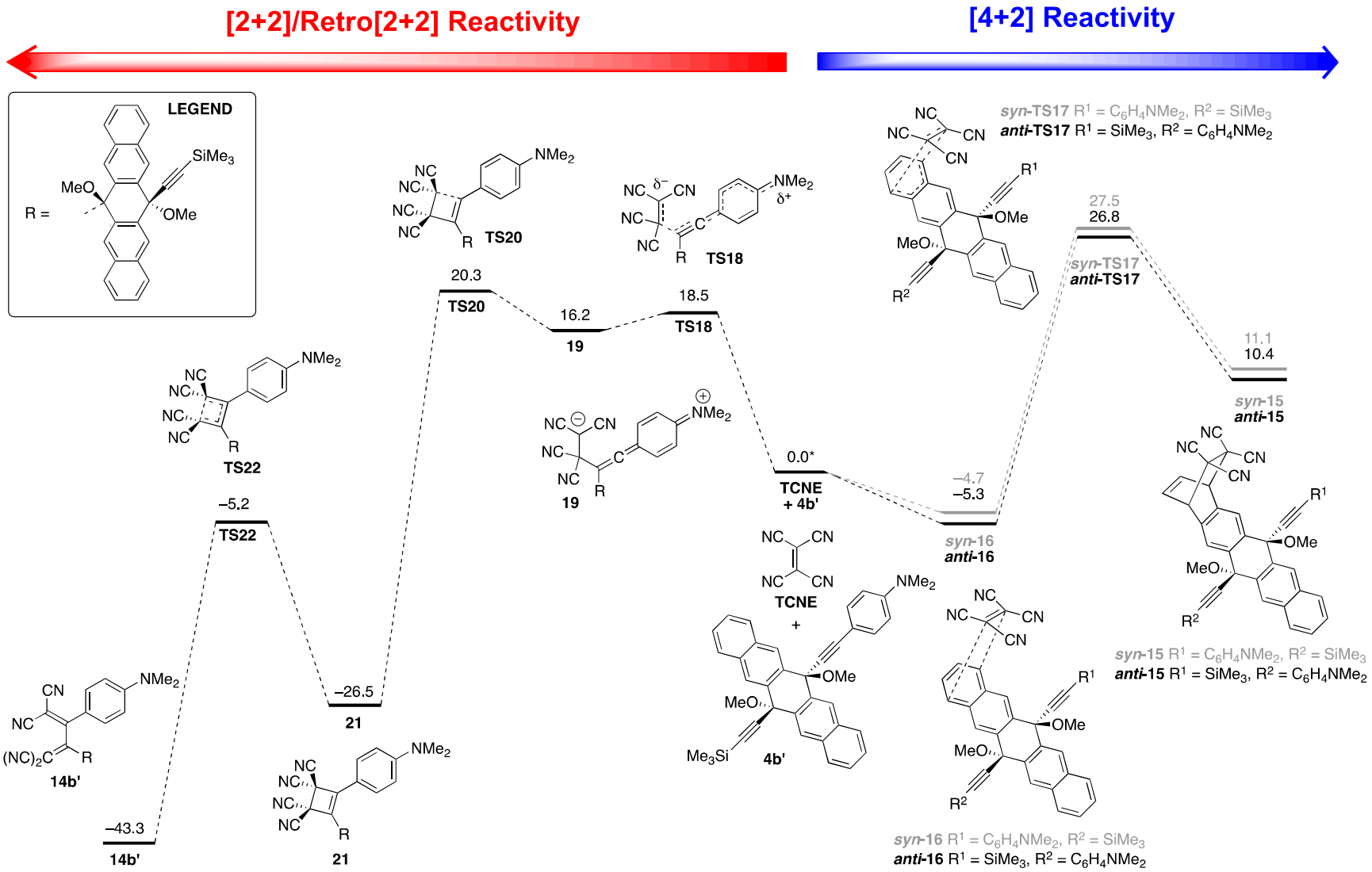

Figure 7. DFT calculated energy profile using B3LYP/6-31G(d) for reaction of TCNE with pentacene **4b'** illustrating the origin of the preference for the formal [2+2]/retro[2+2] pathway versus the [4+2] pathway.

The sensitivity of the pentacene core to reactions with TCNE suggested the use of dehydropentacene precursor **4b** in place of pentacene **1b** (Scheme 4) towards achieving [2+2] reactivity with the alkyne instead of [4+2] reactivity with the pentacene to form product **14b'** instead of ***syn/anti*-15**, respectively. Examination of this hypothesis with DFT (structures **14**–**22**, Figure 7) supports the feasibility for TCNE to preferentially react with the alkyne in a [2+2] manner instead of reacting with the acene in [4+2] fashion by using dehydropentacene **4b** instead of pentacene **1b**. Comparing the relevant transition states, the energy barrier associated with the [4+2] pathway (***anti*-TS17**) is 6.5 kcal/mol higher than the highest energy barrier along the [2+2]/[4+2] pathway (**TS20**).

Experimentally, dehydropentacene **4b** reacts cleanly with TCNE to provide an intensely red coloured product. While mass spectral analysis was consistent with formation of the expected product **14b**, ^{1}H and ^{13}C NMR spectra of the product clearly shows two non-equivalent naphthyl moieties.[39] This suggested that either an alternative product had formed, or that there is restricted or slow rotation on the NMR timescale with regard to the position of the aniline group relative to the two naphthyl moieties. Indeed, the later premise is supported by X-ray crystallography (Figure 8), which provided unambiguous proof of the structure of the isolated product and shows the aniline group located above one of the naphthyl moieties with contacts as short as 3.0–3.4 Å (carbons of aniline ring to plane of naphthyl ring). Unfortunately, attempted conversion of **14b** to **23b** under typical aromatization conditions using $SnCl_2 \bullet 2H_2O$ (with and without H_2SO_4), was not successful and attempts with forcing conditions (reflux) resulted in decomposition.

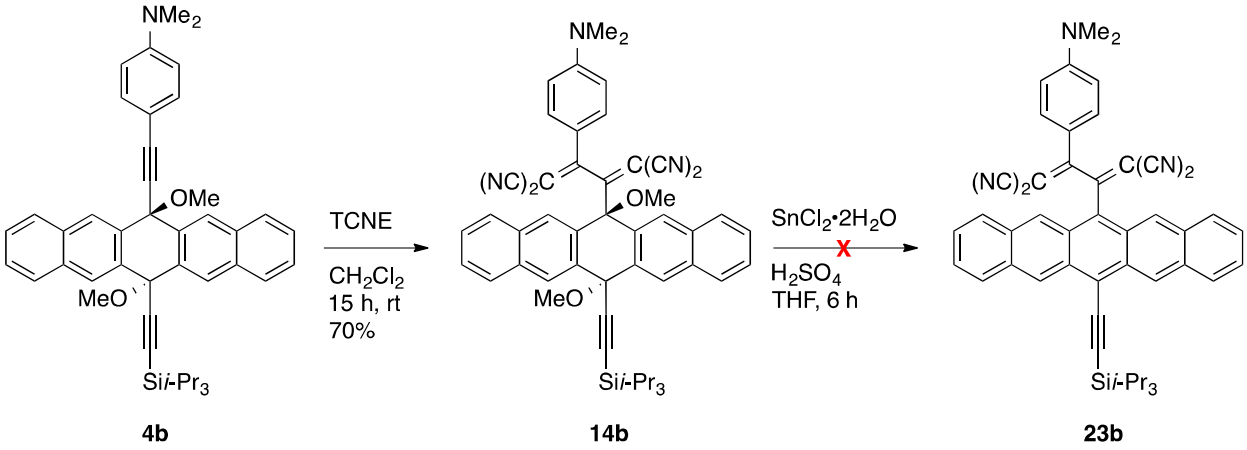

Scheme 4. Attempted synthesis of **23b** from compound **14b**.

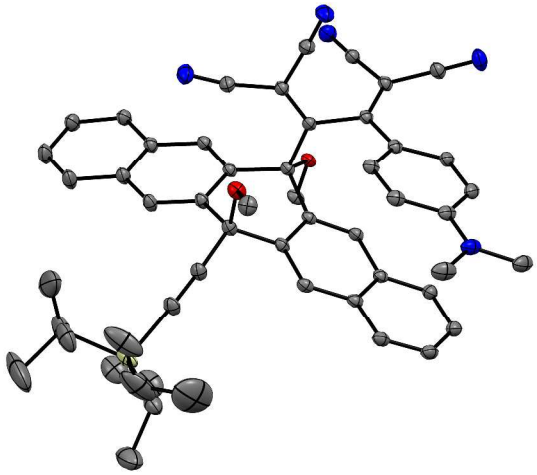

Figure 8. ORTEP representation of the X-ray crystallographic structure of **14b**. Hydrogen atom not shown, and non-hydrogen atoms are represented by Gaussian ellipsoids at the 50% probability level.

In summary, we have developed synthetic methodology that allows for appending strong electron-donating and -withdrawing groups on the pentacene framework and extension of this method to form a "push-pull" pentacene. The presence of a donor and/or acceptor has a significant effect on the electronic make-up of the acenes demonstrated by UV-vis and cyclic voltammetry analysis. This electronic influence also affects chemical reactivity, as

demonstrated by reactions of **1d** and **4b** with TCNE. The origin of the difference in reactivity towards TCNE with various pentacene derivatives is revealed using DFT calculations and provides design principles towards controlling [4+2] over [2+2] reactivity. This study contributes to paving the way to stronger donor-acceptor functionalized acenes for organic electronic applications which may be of use for improved solar cell performance based on singlet fission processes where charge transfer states are believed to play an important role.[49]

Experimental section

General experimental methods

Reagents were purchased in reagent grade from commercial suppliers and used without further purification. Compounds **1d,e**,[30] **2a,b**, and **6b**[20a] were synthesized via reported procedures. THF and benzene were distilled from sodium/benzophenone ketyl. CH_2Cl_2 and MeCN were distilled from CaH_2. Anhydrous $MgSO_4$ was used as the drying agent after aqueous work-up. Evaporation and concentration *in vacuo* was done at water-aspirator pressure. All reactions were performed in standard, dry glassware under an inert atmosphere of nitrogen or argon. Column chromatography: silica gel-60 (230–400 mesh). Thin Layer Chromatography (TLC): pre-coated plastic sheets covered with 0.20 mm silica gel with fluorescent indicator UV 254 nm; visualization by UV light or $KMnO_4$ stain. Melting points are uncorrected. ^{1}H- and ^{13}C-NMR spectra were collected at 27 °C in $CDCl_3$; solvent peaks (7.24 ppm for ^{1}H and 77.0 ppm for ^{13}C) as reference. Coupling constants are reported as observed (±0.5 Hz). UV-vis absorption spectra were acquired at rt using a Varian Cary 400 Scan Spectrometer; λ_{max} in nm (ε in L•mol^{-1}•cm^{-1}). Emission spectra were recorded using Photon Technology International (PTI) MP1 Fluorescence system. For mass spectral analyses, low-resolution data are provided in cases when M^+ is not the base peak; otherwise, only high-resolution data are provided. The samples for ESI

mass spectrometry were dissolved in $ClCH_2CH_2Cl$ and made use of a 3:1 MeOH/toluene mixture as the carrier solvent. MALDI mass spectrometry used the matrix *trans*-2-[3-(4-*tert*-butylphenyl)-2-methyl-2-propenylidene]malononitrile (DCTB).

Differential scanning calorimetry (DSC) measurements were measured on a Perkin Elmer Pyris 1 DSC instrument. Thermogravometric analyses (TGA) were carried out on a Perkin Elmer Pyris 1 TGA instrument. All thermal analyses were carried out under a flow of nitrogen with a heating rate of 10 °C/min. Thermal decomposition temperature as measured by TGA (as sample weight loss) are reported as T_d in which the temperature listed corresponds to the intersection of the tangent lines of the baseline and the edge of the peak corresponding to the first significant weight loss, typically >5%. Melting points from DSC analysis are reported as the peak maxima, except in cases when the sample decomposed, in which case the onset temperature of the decomposition exothermic peak is reported, as well as the exothermic maxima corresponding to the decomposition.

Cyclic voltammetry experiments were done using a Bioanalytical Systems, Inc. (BASi) Epsilon Rotating-Disk Electrode (Model RDE-2). Data was analyzed by BASi Epsilon-EC Ver. 2.00.71–USB, BASi ComServer Ver. 1.03 on a PC computer. A three-electrode cell was used, using a platinum disk working electrode and a platinum wire counter electrode. Silver/silver ion (Ag in 0.1 M $AgNO_3$, 0.1 M *n*-Bu_4NPF_6 solution in MeCN) was used as a reference electrode. Ferrocene/ferrocenium (Fc/Fc^+) was used as an internal standard. The potential values (E) were calculated using the following equation (except where otherwise noted): $E = (E_{pc} + E_{pa})/2$, where E_{pc} and E_{pa} correspond to the cathodic and anodic peak potentials, respectively. The potential values obtained in reference to Ag/Ag^+ were converted to potentials vs. ferrocene/ferrocenium (Fc/Fc^+). Solution cyclic voltammetry was performed in ca. 1 mM solution of pentacene

derivatives in benzene/MeCN (3:1 v/v) containing 0.1 M *n*-Bu_4NPF_6 as supporting electrolyte at a scan rate of 150 mV•s^{-1}, except where noted otherwise. All solutions were deoxygenated with N_2 before each experiment and a blanket of N_2 was used over the solution during the experiment. The working electrode was polished with 0.05 μm alumina polish prior to each scan. Solutions of pentacenes **1a–e** and **6b** were analyzed with a scanning window of 1.0 V to –2.0 V (vs Ag/Ag^+), while pentacene **6a** was analyzed with a scanning window of 1.0 V to –2.2 V (vs Ag/Ag^+).

X-ray data for **1b**•0.5CH_2Cl_2 (CCDC 865682), **6a** (CCDC 865683), **8d** (CCDC 865684) and **14b** (CCDC 865403) have been deposited at the Cambridge Crystallographic Data Centre (CCDC), 12 Union Road, Cambridge CB21EZ, UK; fax: (+44)122-333-6033. These data can be obtained free of charge from The Cambridge Crystallographic Data Centre via the Internet at www.ccdc.cam.ac.uk/data_request/cif using the CCDC numbers given above.

X-ray crystallographic data

Data for 1b. Crystals suitable for X-ray crystallographic analysis were obtained from a solution of **1b** in CH_2Cl_2 which had been layered by acetone and allowed to slowly evaporate at 4 °C. X-ray data for **1b**•0.5CH_2Cl_2: $C_{43}H_{43}ClNSi$•0.5CH_2Cl_2, M_r = 644.34; crystal dimensions (mm) 0.39 × 0.19 × 0.08; monoclinic space group $P2_1/c$ (No. 14); a = 9.2434(3) Å, b = 26.2155(8) Å, c = 14.8529(5) Å; β = 91.4551(4)°; V = 3598.0(2) $Å^3$; Z = 4; ρ_{calcd} = 1.189 g cm^{-3}; μ = 0.171 mm^{-1}; λ = 0.71073 Å; T = –100 °C; $2\theta_{max}$ = 52.82°; total data collected = 28699; R_1 = 0.0423 [5794 observed reflections with $F_o^2 \geq 2\sigma(F_o^2)$]; wR_2 = 0.1122 for 426 variables, 0 restraints, and 7395 unique reflections; residual electron density = 0.551 and –0.568 e $Å^{-3}$. (CCDC 865682).

Data for 6a. Crystals suitable for X-ray crystallographic analysis were obtained from a solution of **6a** in CH_2Cl_2 which had been layered by acetone and allowed to slowly evaporate at 4 °C. X-ray data for **6a**: $C_{50}H_{46}N_2O_2$, M_r = 706.89; crystal dimensions (mm) 0.46 × 0.15 × 0.10; triclinic

space group P-1 (No. 2); a = 11.3590(8) Å, b = 12.7835(8) Å, c = 14.8035(10) Å; α = 74.2113(8)°, β = 72.9134(8)°, γ = 76.7681(8)°; V = 1951.1(2) Å^3; Z = 2; ρ_{calcd} = 1.203 g cm^{-3}; μ = 0.073 mm^{-1}; λ = 0.71073 Å; T = –100 °C; $2\theta_{max}$ = 51.56°; total data collected = 14731; R_1 = 0.0444 [5021 observed reflections with $F_o^2 \geq 2\sigma(F_o^2)$]; wR_2 = 0.1251 for 487 variables, 0 restraints, and 7477 unique reflections; residual electron density = 0.167 and –0.213 e Å^{-3}. (CCDC 865683).

Data for 8d. Crystals suitable for X-ray crystallographic analysis were obtained from a solution of **8d** in $CHCl_3$ which was allowed to slowly evaporate at 4 °C. X-ray data for **8d**: $C_{48}H_{40}N_4OSi$, M_r = 716.93; crystal dimensions (mm) 0.40 × 0.11 × 0.07; monoclinic space group $P2_1/c$ (No. 14); a = 15.9034(13) Å, b = 12.3331(10) Å, c = 20.8200(18) Å; β = 103.3580(13)°; V = 3973.1(6) Å^3; Z = 4; ρ_{calcd} = 1.199 g cm^{-3}; μ = 0.100 mm^{-1}; λ = 0.71073 Å; T = –100 °C; $2\theta_{max}$ = 51.46°; total data collected = 29103; R_1 = 0.0467 [4791 observed reflections with $F_o^2 \geq 2\sigma(F_o^2)$]; wR_2 = 0.1118 for 487 variables, 0 restraints, and 7580 unique reflections; residual electron density = 0.207 and –0.305 e Å^{-3}. (CCDC 865684).

Data for 14b. Crystals suitable for X-ray crystallographic analysis were obtained from a solution of **14b** in hexanes/CH_2Cl_2 (3:1) which was allowed to slowly evaporate at 4 °C. X-ray data for **14b**: $C_{51}H_{49}N_5O_2Si$, M_r = 792.04; crystal dimensions (mm) 0.42 × 0.222 × 0.11; triclinic space group P-1 (No. 2); a = 11.8561(6) Å, b = 15.0323(10) Å, c = 15.1075(10) Å, α = 115.327(7)°, β = 91.628(5)°, γ = 103.478(5)°, V = 2341.4(3); Z = 2; ρ_{calcd} = 1.123 g cm^{-3}; μ = 0.774 mm^{-1}; T = 174(3) K; $2\theta_{max}$ = 147.08°; total data collected = 16660; R_1 = 0.0607 [9138 observed reflections with $F_o^2 \geq 2\sigma(F_o^2)$]; wR_2 = 0.1873 for 566 variables, 9138 unique reflections, and 11 restraints; residual electron density = 0.59 and –0.44 e Å^{-3}. (CCDC 865403). Three disordered triisopropyl

groups were refined with the following occupancies: C4–C5, 30:70; C7–C8, 59:41; C10–C11, 51:49. In addition, a residual electron density pattern indicated a strongly disordered solvent molecule, likely CH_2Cl_2. All attempts to model and resolve this solvent molecule and the related disorder failed. Therefore finally the "solvent mask" option of OLEX2 was used to mask this region for refinement.[50]

Compound 1a: To a solution of **4a** (0.104 g, 0.129 mmol) in dry THF (10 mL) that had been deoxygenated by bubbling argon for 5 min was added $SnCl_2 \cdot 2H_2O$ (0.101 g, 0.448 mmol). The solution was stirred at rt for 5 h, poured onto a pad of silica gel, eluted with 1:1 CH_2Cl_2/hexanes, and the solvent was removed *in vacuo*. Column chromatography (silica gel, 3:2 CH_2Cl_2/hexanes) afforded **1a** (0.080 g, 84%) as a deep blue solid. R_f = 0.67 (3:2 CH_2Cl_2/hexanes). UV-vis (CH_2Cl_2) λ_{max} (ε): 274 (sh, 21 300), 315 (181 000), 336 (sh, 21 700), 394 (11 000), 440 (2 660), 495 (3 580), 626 (sh, 12 200), 674 (18 400) nm. No significant emission in CH_2Cl_2. IR ($CDCl_3$ microscope): 3048 (w), 2955 (s), 2924 (s), 2863 (s), 2169 (s), 2120 (m), 1604 (s), 1526 (s) cm^{-1}. ^1H NMR (500 MHz, $CDCl_3$): δ 9.26 (broad s, 4H), 8.08–7.98 (m, 2H), 7.98–7.89 (m, 2H), 7.73 (d, J = 8.7 Hz, 2H), 7.44–7.32 (m, 4H), 6.72 (d, J = 8.8 Hz, 2H), 3.34 (t, J = 7.5 Hz, 4H), 1.70–1.58 (m, 4H), 1.44–1.20 (m, 33H), 0.98–0.89 (m, 6H). ^{13}C NMR (100 MHz, $CDCl_3$): δ 148.4, 133.2, 132.2, 131.9, 130.8, 129.8, 128.7, 128.6, 126.3, 126.2, 125.8, 125.6, 119.7, 116.5, 111.4, 109.0, 107.2, 106.2, 105.1, 86.4, 51.1, 31.7, 27.3, 26.8, 22.7, 19.0, 14.1, 11.7. ESI HRMS *m/z* calcd. for $C_{53}H_{64}NSi$ ($[M + H]^+$) 742.4803, found 742.4787. TGA: T_d ≈ 410 °C. DSC: decomposition, 177 °C (onset), 181 °C (peak).

Compound 1b: To a solution of **4b** (0.121 g, 0.182 mmol) in dry THF (10 mL) that had been deoxygenated by bubbling argon for 5 min was added $SnCl_2 \cdot 2H_2O$ (0.204 g, 0.904 mmol). The solution was stirred at rt for 5 h, poured onto a pad of silica gel, eluted with 2:1 CH_2Cl_2/hexanes,

and the solvent was removed *in vacuo*. Column chromatography (silica gel, 2:1 CH_2Cl_2/hexanes) afforded **1b** (0.097 g, 89%) as a deep blue solid. R_f = 0.80 (2:1 CH_2Cl_2/hexanes). UV-vis (CH_2Cl_2) λ_{max} (ε): 275 (sh, 30 900), 314 (272 000), 389 (16 200), 440 (4 640), 481 (4 550), 619 (16 100), 668 (25 200) nm. No significant emission in CH_2Cl_2. IR (CH_2Cl_2 cast film): 3046 (w), 2941 (m), 2890 (w), 2863 (m), 2170 (m), 2120 (w), 1606 (s), 1525 (m), 1362 (m) cm^{-1}. ^1H NMR (500 MHz, $CDCl_3$): δ 9.25 (s, 2H), 9.24 (s, 2H), 8.04–7.98 (m, 4H), 7.74 (d, J = 8.6 Hz, 2H), 7.42–7.35 (m, 4H), 6.76 (d, J = 8.7 Hz, 2H), 3.03 (s, 6H), 1.45–1.34 (m, 21H). ^{13}C NMR (125 MHz, $CDCl_3$): δ 150.4, 133.0, 132.2, 131.9, 130.8, 129.8, 128.7, 128.6, 126.3, 126.2, 125.8, 125.6, 119.5, 116.7, 111.9, 110.3, 106.8, 106.2, 105.1, 86.6, 40.2, 19.0, 11.7. ^{13}C NMR (APT, 125 MHz, $CDCl_3$): δ 150.4 (C), 133.0 (CH), 132.2 (C), 131.9 (C), 130.8 (C), 129.8 (C), 128.7 (CH), 128.6 (CH), 126.3 (CH), 126.2 (CH), 125.8 (CH), 125.6 (CH), 119.5 (C), 116.7 (C), 111.9 (CH), 110.3 (C), 106.8 (C), 106.2 (C), 105.1 (C), 86.6 (C), 40.2 (CH_3), 19.0 (CH_3), 11.7 (CH). ESI HRMS *m/z* calcd. for $C_{43}H_{44}NSi$ ($[M + H]^+$) 602.3238, found 602.3221. TGA: $T_d \approx 430$ °C. DSC: decomposition, 162 °C (onset), 164 °C (peak).

Compound 1c: To a solution of **4c** (0.105 g, 0.157 mmol) in dry THF (7 mL) that had been deoxygenated by bubbling N_2 for 5 min was added a solution of $SnCl_2 \cdot 2H_2O$ (0.082 g, 0.36 mmol) in THF (7 mL). The solution was stirred at rt for 3 h, poured onto a pad of silica gel, eluted with 1:1 hexanes/CH_2Cl_2, and the solvent was removed *in vacuo*. Column chromatography (silica gel, 1:1 hexanes/CH_2Cl_2) afforded **1c** (0.053 g, 56%) as a green solid. R_f = 0.50 (1:1 hexanes/CH_2Cl_2). UV-vis (CH_2Cl_2) λ_{max} (ε): 274 (29 700), 313 (255 000), 347 (14 600), 395 (14 600), 441 (7 090), 616 (14 400), 666 (22 900) nm. No significant emission in CH_2Cl_2. IR ($CHCl_3$, cast) 3048 (w), 2942 (m), 2890 (w), 2864 (m), 2185 (w), 2124 (w), 1589

(m), 1513 (m), 1337 (s) cm^{-1}. ^1H NMR (500 MHz, $CDCl_3$): δ 8.94 (s, 2H), 8.54 (s, 2H), 8.09 (d, J = 8.4 Hz, 2H), 7.75 (d, J = 8.5 Hz, 2H), 7.62 (d, J = 8.5 Hz, 2H), 7.46 (d, J = 8.3 Hz, 2H), 7.32 (t, J = 7.2 Hz, 2H), 7.26 (t, J = 7.2 Hz, 2H), 1.46–1.36 (m, 21H). gCOSY NMR (500 MHz, $CDCl_3$): δ 8.94 ↔ 7.75; 8.54 ↔ 7.62; 8.09 ↔ 7.46; 7.75 ↔ 8.94, 7.32; 7.62 ↔ 8.54, 7.26; 7.46 ↔ 8.09; 7.32 ↔ 7.75; 7.26 ↔ 7.62. ^{13}C NMR (125 MHz, $CDCl_3$): δ 146.6, 132.1, 131.9, 131.7, 130.1, 130.0, 129.8, 128.5, 128.3, 126.4, 126.1, 125.9, 125.0, 123.5, 119.6, 115.9, 107.8, 104.6, 101.9, 92.9, 19.0, 11.7. ^{13}C NMR (APT, 125 MHz, $CDCl_3$): δ 146.6 (C), 132.1 (C), 131.9 (C), 131.7 (CH), 130.1 (C), 130.0 (C), 129.8 (C), 128.5 (CH), 128.3 (CH), 126.4 (CH), 126.1 (CH), 125.9 (CH), 125.0 (CH), 123.5 (CH), 119.6 (C), 115.9 (C), 107.8 (C), 104.6 (C), 101.9 (C), 92.9 (C), 19.0 (CH_3), 11.7 (CH). MALDI HRMS *m/z* calcd. for $C_{41}H_{37}NO_2Si$ (M^+) 603.2588, found 603.2590. TGA: $T_d \approx 330$ °C. DSC: decomposition, 197 °C (onset), 225 °C (peak).

Compound 3a: To a solution of $BnEt_3NICl_2$[51] (2.81 g, 7.203 mmol) in $CHCl_3$ (30 mL) and MeOH (15 mL) was added *N*,*N*-dihexylaniline (2.00 g, 7.65 mmol) and $CaCO_3$ (2.41 g, 24.1 mmol). The flask was wrapped in aluminum foil to protect from light and the reaction mixture was stirred for 48 h at rt. The solution was filtered through a pad of Celite® with CH_2Cl_2 and the solvent was removed *in vacuo*. Column chromatography (silica gel, 10:1 hexanes/CH_2Cl_2) afforded **3a** (2.51 g, 90%) as a clear yellow liquid. R_f = 0.43 (10:1 CH_2Cl_2/hexanes). IR (CH_2Cl_2 cast film): 3086 (w), 2955 (s), 2928 (s), 2857 (m), 1589 (s), 1499 (s) cm^{-1}. ^1H NMR (400 MHz, $CDCl_3$): δ 7.44 (d, J = 8.6 Hz, 2H), 6.44 (d, J = 8.9 Hz, 2H), 3.24 (t, J = 7.7 Hz, 4H), 1.58 (quintet, J = 6.7 Hz, 4H), 1.42–1.28 (m, 12H), 0.99–0.89 (m, 6H). ^{13}C NMR (100 MHz, $CDCl_3$): δ 147.5, 137.5, 113.9, 75.3, 50.9, 31.7, 27.0, 26.7, 22.6, 14.0. ^{13}C NMR (APT, 100 MHz, $CDCl_3$): δ 147.5 (C), 137.5 (CH), 113.9 (CH), 75.3 (C), 50.9 (CH_2), 31.7 (CH_2), 27.0 (CH_2), 26.7

(CH_2), 22.6 (CH_2), 14.0 (CH_3). EI MS *m/z* 387.1 (M^+, 56), 316.1 ([M – C_5H_{11}]$^+$, 100). EI HRMS *m/z* calcd. for $C_{18}H_{30}IN$ (M^+) 387.1423, found 387.1422.

Compound 3b.[52] 4-Iodo-*N*,*N*-dimethylaniline was synthesized analogously to **3a** (*vide supra*). Spectroscopic data of **3b** was in agreement with that reported.[52b,d]

Compound 4a: To a solution of **2a** (0.288 g, 0.527 mmol) and **3a** (0.331 g, 0.855 mmol) in THF (7 mL) and diisopropylamine (5.0 mL, 3.6 g, 35 mmol) which had been deoxygenated with argon for 10 min was added $Pd(PPh_3)_4$ (0.030 g, 0.026 mmol) and CuCl (0.005 g, 0.05 mmol) and the solution was further deoxygenated for 5 min. The solution was stirred for 20 h at 45–55 °C before being poured into satd. aq. NH_4Cl (200 mL). H_2O (100 mL) was added and the mixture was extracted with CH_2Cl_2 (80 mL, 50 mL). The organic phase was washed with 5% aq. NH_4Cl (200 mL), dried ($MgSO_4$), filtered, and the solvent removed *in vacuo*. Column chromatography (silica gel, 5:4 CH_2Cl_2/hexanes, column wrapped in aluminum foil to exclude light) afforded **4a** (0.119 g, 28%) as a brown oil. R_f = 0.38 (5:4 CH_2Cl_2/hexanes). IR (CH_2Cl_2 cast film): 3054 (w), 2931 (s), 2220 (m), 2169 (vw), 1607 (s), 1519 (s) 1081 (m), 1062 (m) cm^{-1}. ^1H NMR (500 MHz, $CDCl_3$): δ 8.71 (s, 2H), 8.54 (s, 2H), 8.02–7.97 (m, 2H), 7.97–7.92 (m, 2H), 7.59–7.51 (m, 4H), 7.23 (d, *J* = 9.0 Hz, 2H), 6.46 (d, *J* = 9.1 Hz, 2H), 3.21 (t, *J* = 7.7 Hz, 4H), 3.11 (s, 3H), 3.07 (s, 3H), 1.57–1.47 (m, 4H), 1.34–1.25 (m, 12H), 1.25–1.19 (m, 21H), 0.91–0.86 (m, 6H). ^{13}C NMR (125 MHz, $CDCl_3$): δ 147.8, 134.8, 133.5, 133.4, 132.9, 132.8, 128.2, 128.0, 126.9, 126.6, 126.4, 110.9, 108.3, 106.3, 90.8, 88.6, 88.1, 75.7, 74.1, 52.1, 51.9, 50.9, 31.6, 27.1, 26.7, 22.6, 18.7, 14.0, 11.4 (one signal coincident or not observed). ^{13}C NMR (APT, 125 MHz, $CDCl_3$): δ 147.8 (C), 134.8 (C), 133.5 (C), 133.4 (CH), 132.9 (C), 132.8 (CH), 128.2 (CH), 128.0 (CH), 126.9 (CH), 126.6 (CH), 126.4 (CH), 110.9 (CH), 108.3 (C), 106.3 (C), 90.8 (C), 88.6 (C), 88.1 (C), 75.7 (C), 74.1 (C), 52.1 (CH_3), 51.9 (CH_3), 50.9 (CH_2), 31.6 (CH_2), 27.1

(CH_2), 26.7 (CH_2), 22.6 (CH_2), 18.7 (CH_3), 14.0 (CH_3), 11.4 (CH) (one signal coincident or not observed). ESI MS *m/z* 804.5 ($[M + H]^+$, 100), 772.5 ($[M – OMe]^+$, 66). ESI HRMS *m/z* calcd. for $C_{55}H_{70}NO_2Si$ ($[M + H]^+$) 804.5170, found 804.5155.

Compound 4b: To a solution of **2a** (0.285 g, 0.524 mmol) and **3b** (0.152 g, 0.614 mmol) in THF (5 mL) and diisopropylamine (3 mL, 2 g, 0.2 mmol) which had been deoxygenated with argon for 10 min was added $Pd(PPh_3)_4$ (0.030 g, 0.026 mmol) and CuCl (0.005 g, 0.05 mmol) and the solution was further deoxygenated for 5 min. The solution was stirred for 20 h at rt before being poured into satd. aq. NH_4Cl (150 mL). H_2O (50 mL) was added and the mixture was extracted with CH_2Cl_2 (80 mL, 50 mL). The organic phase was washed with 5% aq. NH_4Cl (150 mL), satd. aq. NaCl (150 mL), dried ($MgSO_4$), filtered, and the solvent removed *in vacuo*. The residue was dissolved in a small amount of EtOAc (ca. 1 mL) to which MeOH (ca. 30 mL) was added. The solution was cooled to –78 °C, filtered, and the solid was washed with MeOH (3 × 5 mL) to afford **4b** (0.254 g, 73%) as a white solid that is unstable to silica gel. IR (microscope): 3052 (w), 2942 (s), 2891 (m), 2864 (s), 2829 (w), 2816 (w), 2223 (m), 2164 (vw), 1609 (s) cm^{-1}. ^1H NMR (500 MHz, $CDCl_3$): δ 8.70 (s, 2H), 8.50 (s, 2H), 8.00–7.95 (m, 2H), 7.94–7.88 (m, 2H), 7.56–7.49 (m, 4H), 7.22 (d, *J* = 9.1 Hz, 2H), 6.50 (d, *J* = 9.1 Hz, 2H), 3.09 (s, 3H), 3.04 (s, 3H), 2.89 (s, 6H), 1.27–1.17 (m, 21H). ^{13}C NMR (125 MHz, $CDCl_3$): δ 150.9, 134.7, 133.5, 133.3, 132.8, 128.21, 128.16, 128.1, 126.9, 126.7, 126.5, 111.5, 109.8, 106.0, 91.3, 89.1, 87.6, 75.9, 73.9, 52.1, 51.9, 40.1, 18.8, 11.4 (one signal coincident or not observed). ESI MS *m/z* 686.3 ($[M + Na]^+$, 3), 664.4 ($[M + H]^+$, 2), 632.3 ($[M – OMe]^+$, 100). ESI HRMS *m/z* calcd. for $C_{45}H_{49}NO_2SiNa$ ($[M + Na]^+$) 686.3425, found 686.3416.

Compound 4c: To a solution of **2a** (0.410 g, 0.753 mmol) and **3c** (0.171 g, 0.687 mmol) in THF (6 mL) and diisopropylamine (3 mL, 2 g, 0.2 mmol) which had been degassed for 10 min with

argon was added $Pd(PPh_3)_4$ (0.039 g, 0.34 mmol) and CuCl (0.011 g, 0.11 mmol). The reaction mixture was further deoxygenated with argon for an additional 2 min. The solution was stirred for 20 h at rt before being poured into satd. aq. NH_4Cl (150 mL). H_2O (50 mL) was added and the mixture was extracted with CH_2Cl_2 (80 mL, 50 mL). The organic phase was washed with 5% aq. NH_4Cl (150 mL), satd. aq. NaCl (150 mL), dried ($MgSO_4$), filtered, and the solvent removed *in vacuo*. Column chromatography (silica gel, CH_2Cl_2) afforded **4c** (0.412 g, 90%) as an off white foamy solid. R_f = 0.73 (CH_2Cl_2), 0.67 (2:1 hexanes/EtOAc), 0.24 (9:1 hexanes/EtOAc). IR (CH_2Cl_2 cast film): 3056 (w), 2943 (m), 2892 (w), 2865 (m), 2230 (vw), 2170 (vw), 1594 (m), 1520 (s), 1344 (s) cm^{-1}. ^1H NMR (500 MHz, $CDCl_3$): δ 8.78 (s, 2H), 8.45 (s, 2H), 8.04 (d, J = 8.2 Hz, 2H), 8.02–7.97 (m, 2H), 7.97–7.91 (m, 2H), 7.61–7.54 (m, 4H), 7.43 (d, J = 8.2 Hz, 2H), 3.13 (s, 3H), 3.11 (s, 3H), 1.35–1.24 (m, 21H). ^{13}C NMR (125 MHz, $CDCl_3$): δ 147.0, 133.6, 133.4, 133.0, 132.8, 132.3, 129.8, 128.5, 128.3, 128.1, 127.1, 126.92, 126.85, 123.2, 104.3, 97.2, 93.0, 83.5, 76.5, 73.3, 52.2, 51.9, 18.8, 11.4. ^{13}C NMR (APT, 125 MHz, $CDCl_3$): δ 147.0 (C), 133.6 (C), 133.4 (C), 132.9 (C), 132.8 (C), 132.3 (CH), 129.8 (C), 128.5 (CH), 128.3 (CH), 128.1 (CH), 127.1 (CH), 126.92 (CH), 126.86 (CH), 123.2 (CH), 104.3 (C), 97.2 (C), 93.0 (C), 83.5 (C), 76.5 (C), 73.3 (C), 52.2 (CH_3), 52.0 (CH_3), 18.8 (CH_3), 11.4 (CH). MALDI HRMS *m/z* calcd. for $C_{43}H_{43}NO_4Si$ (M^+) 665.2956, found 665.2958. Anal. calcd. for $C_{43}H_{43}NO_4Si$: C, 77.56; H, 6.51; N, 2.10. Found: C, 77.34; H, 6.35; N, 2.21.

Compound 4d: To a solution of **2b** (0.585 g, 0.993 mmol) and **3c** (0.344 g, 1.38 mmol) in THF (7 mL) and diisopropylamine (5.0 mL, 3.6 g, 35 mmol) which had been deoxygenated for 10 min with argon was added $Pd(PPh_3)_4$ (0.030 g, 0.026 mmol) and CuCl (0.005 g, 0.05 mmol). The reaction mixture was further deoxygenated for an additional 2 min. The solution was stirred for 12 h at 40 °C before being poured into satd. aq. NH_4Cl (150 mL). H_2O (100 mL) was added and

the mixture was extracted with CH_2Cl_2 (80 mL, 50 mL). The organic phase was washed with 5% aq. NH_4Cl (150 mL), dried ($MgSO_4$), filtered, and the solvent removed *in vacuo*. Column chromatography (silica gel, 2:1 CH_2Cl_2/hexanes) afforded **4d** (0.578 g, 82%) as an off white foamy solid. R_f = 0.65 (2:1 CH_2Cl_2/hexanes). IR (microscope): 3056 (w), 2952 (s), 2928 (m), 2896 (m), 2867 (m), 2230 (w), 2169 (w), 1595 (s), 1520 (s) cm^{-1}. ^1H NMR (500 MHz, $CDCl_3$): δ 8.70 (s, 2H), 8.44 (s, 2H), 8.03 (d, *J* = 9.0 Hz, 2H), 8.01–7.96 (m, 2H), 7.96–7.90 (m, 2H), 7.59–7.54 (m, 4H), 7.42 (d, *J* = 9.1 Hz, 2H), 3.10 (s, 3H), 3.06 (s, 3H), 2.08 (nonet, *J* = 6.7 Hz, 3H), 1.11 (d, *J* = 6.6 Hz, 18H), 0.86 (d, *J* = 7.0 Hz, 6H). ^{13}C NMR (125 MHz, $CDCl_3$): δ 147.0, 133.6, 133.4, 133.0, 132.8, 132.3, 129.8, 128.5, 128.2, 128.1, 127.1, 127.0, 123.3, 104.4, 97.2, 95.5, 83.5, 76.3, 73.3, 52.2, 52.0, 26.5, 25.3, 25.2, (one signal coincident or not observed). ESI MS *m/z* 730.3 ($[M + Na]^+$, 48), 676.3 ($[M – OMe]^+$, 100). ESI HRMS *m/z* calcd. for $C_{46}H_{49}NO_4SiNa$ ($[M + Na]^+$) 730.3323, found 730.3311.

Compound 4e: To a solution of **4d** (0.566 g, 0.799 mmol) in THF (80 mL) at –78 °C was added TBAF (1.0 M in THF, 0.82 mL, 0.82 mmol). The solution was stirred for 1 h at –78 °C before warming the solution to –15 °C and stirring for an additional 30 min. The reaction mixture was then poured into satd. aq. NH_4Cl (150 mL). H_2O (100 mL) was added and the mixture was extracted with CH_2Cl_2 (150 mL, 100 mL). The organic phase was washed with 5% aq. NH_4Cl (150 mL), dried ($MgSO_4$), filtered, and the solvent removed *in vacuo*. Column chromatography (silica gel, 4:1 hexanes/EtOAc) afforded **4e** (0.354 g, 87%) as an off white foamy solid. R_f = 0.31 (4:1 hexanes/EtOAc), 0.50 (CH_2Cl_2). IR (CH_2Cl_2 cast film): 3290 (m), 2056 (w), 2936 (w), 2230 (vw), 2117 (vw), 1594 (s), 1519 (s) cm^{-1}. ^1H NMR (500 MHz, $CDCl_3$): δ 8.64 (s, 2H), 8.50 (s, 2H), 8.09 (d, *J* = 9.0 Hz, 2H), 8.03–7.96 (m, 4H), 7.60–7.54 (m, 4H), 7.51 (d, *J* = 9.0 Hz, 2H), 3.12 (s, 1H), 3.11 (s, 3H), 3.08 (s, 3H). ^{13}C NMR (125 MHz, $CDCl_3$): δ 147.1, 133.4, 133.1,

133.0, 132.7, 132.4, 129.5, 128.3, 128.1, 128.0, 127.3, 127.1, 127.0, 123.4, 96.2, 84.6, 82.4, 78.0, 75.1, 73.9, 52.1, 52.0. ESI MS *m/z* 532.2 ($[M + Na]^+$, 100). HRMS ESI *m/z* calcd. for $C_{34}H_{23}NO_4Na$ ($[M + Na]^+$) 532.1519, found 532.1510.

Compound 5: To a solution of **4e** (0.307 g, 0.602 mmol) and **3a** (0.352 g, 0.909 mmol) in THF (7 mL) and diisopropylamine (5.0 mL, 3.6 g, 36 mmol) which had been deoxygenated for 10 min with argon was added $Pd(PPh_3)_4$ (0.030 g, 0.026 mmol) and CuCl (0.005 g, 0.05 mmol) followed by additional deoxygenation with argon for 5 min. The solution was stirred for 14 h at rt before being poured into satd. aq. NH_4Cl (150 mL). H_2O (100 mL) was added and the mixture was extracted with CH_2Cl_2 (80 mL, 50 mL). The organic phase was washed with 5% aq. NH_4Cl (150 mL), dried ($MgSO_4$), filtered, and the solvent removed *in vacuo*. The crude yellow oil containing **5** was used for the synthesis of **6a** without further purification. HRMS ESI *m/z* calcd. for $C_{52}H_{54}N_2O_4Si$ ($[M + H]^+$) 769.4000, found 769.3984.

Compound 6a: To a solution of crude **5** (0.602 mmol, based on **4e**) in dry THF (20 mL) that had been deoxygenated by bubbling through N_2 for 5 min was added $SnCl_2 \cdot 2H_2O$ (0.271 g, 1.20 mmol). The solution was stirred at rt for 3 h, poured onto a pad of silica gel, eluted with CH_2Cl_2, and the solvent was removed *in vacuo*. Column chromatography (silica gel, CH_2Cl_2) afforded a blue-green solid. The solid was dissolved in minimum CH_2Cl_2 (ca. 6 mL) after which was added hexanes (ca. 50 mL). The suspension was cooled to –78 °C and filtered. The solid was washed with hexanes (5 × 5 mL) to afford **6a** (0.263 g, 62%) as a blue solid. $R_f = 0.99$ (CH_2Cl_2). UV-vis (CH_2Cl_2) λ_{max} (ε): 274 (sh, 38 000), 317 (21 6000), 343 (sh, 30 500), 391 (14 300), 440 (7 600), 497 (8 400), 589 (sh, 9 560), 689 (28 400) nm. No significant emission in CH_2Cl_2. IR ($CHCl_3$, cast) 3045 (w), 2954 (m), 2928 (m), 2857 (w), 2169 (s), 1604 (s), 1590 (s) cm^{-1}. ^1H NMR (500 MHz, $CDCl_3$): δ 8.89 (s, 2H), 8.60 (s, 2H), 8.20 (d, J = 8.5 Hz, 2H), 7.79–7.71 (br s, 4H), 7.70–

7.62 (m, 4H), 7.33–7.26 (m, 4H), 6.73 (d, J = 8.7 Hz, 2H), 3.39 (t, J = 7.7 Hz, 4H), 1.69 (quintet, J = 7.2 Hz, 4H), 1.46–1.34 (m, 12H), 0.95 (t, J = 6.9 Hz, 6H). ^{13}C NMR (125 MHz, $CDCl_3$): δ 148.5, 146.6, 133.3, 132.1, 131.8, 131.6, 130.7, 130.1, 129.2, 128.6, 128.4, 126.5, 125.9, 125.5, 125.1, 123.7, 121.3, 113.9, 111.4, 108.9, 108.3, 101.8, 94.0, 86.8, 51.1, 31.8, 27.3, 26.9, 22.7, 14.1. ESI HRMS *m/z* calcd. for $C_{50}H_{46}N_2O_2$ (M^+) 706.3554, found 706.3542. TGA: $T_d \approx 285$ °C. DSC: decomposition, 152 °C (onset), 177 °C (peak).

Compound 8d: To a solution of **1d** (0.076 g, 0.13 mmol) in CH_2Cl_2 (5 mL) was added tetracyanoethylene (0.012 g, 0.094 mmol). The reaction flask was stirred at rt for 24 h. The solvent was removed *in vacuo* and the residue was purified by column chromatography (silica gel, CH_2Cl_2) to afford **8d** (0.050 g, 74%) as a yellow solid. R_f = 0.70 (CH_2Cl_2). IR ($CHCl_3$ cast film): 3049 (w), 2941 (s), 2892 (m), 2864 (s), 2250 (vw), 2199 (m), 2149 (w), 1604 (s) cm^{-1}. ^{1}H NMR (500 MHz, $CDCl_3$): δ 8.993 (s, 1H), 8.987 (s, 1H), 8.12–8.07 (m, 1H), 8.06–8.00 (m, 1H), 7.77–7.72 (m, 2H), 7.72–7.66 (m, 1H), 7.62–7.54 (m, 3H), 7.54–7.48 (m, 2H), 7.06–7.01 (m, 2H), 5.84 (s, 1H), 5.80 (s, 1H), 3.91 (s, 3H), 1.42–1.24 (m, 21H). ^{13}C NMR (125 MHz, $CDCl_3$): δ 160.8, 133.8, 133.70, 133.67, 132.9, 132.9, 131.9, 130.5, 130.4, 130.3, 129.6, 129.5, 128.5, 127.19, 127.16, 127.14, 127.03, 126.99, 120.9, 119.9, 114.5, 114.1, 110.9, 110.8, 110.4, 110.2, 106.0, 102.9, 100.5, 82.1, 55.5, 51.9, 51.7, 45.8, 45.7, 18.9, 11.4 (two signals coincident or not observed). MALDI MS *m/z* 716.3 (M^+, 5), 588.2 ($[M – (NC)_2C=C(CN)_2]^+$, 100). MALDI HRMS *m/z* calcd. for $C_{48}H_{40}N_4OSi$ (M^+) 716.2966, found 716.2969.

Compound 14b: To a solution of **4b** (0.125 g, 0.188 mmol) in CH_2Cl_2 (9 mL) was added tetracyanoethylene (0.025 g, 0.20 mmol). The reaction flask was stirred at rt for 15 h, poured onto a pad of silica gel, eluted with 3:1 hexanes/EtOAc to collect the red band, and the solvent was removed *in vacuo*. Column chromatography (silica gel, 4:1 hexanes/EtOAc) afforded **14b**

(0.104 g, 70%) as a red solid. ^{1}H NMR (500 MHz, $CDCl_3$): δ ^{1}H NMR (500 MHz, $CDCl_3$): δ 8.64 (s, 1H), 8.61 (s, 1H), 8.23 (br s, 1H), 7.98 (br s, 1H), 7.86 (d, J = 8.1 Hz, 1H), 7.81 (d, J = 8.1 Hz, 2H), 7.71 (br s, 1H), 7.58–7.40 (m, 4H), 7.04 (br s, 2H), 5.95 (d, J = 9.0 Hz, 2H), 3.52 (s, 3H), 3.00 (s, 3H), 2.67 (s, 6H), 1.26–1.19 (m, 21H). ^{13}C NMR (125 MHz, $CDCl_3$): δ 173.8, 162.4, 152.2, 133.8, 133.5, 133.1, 132.9, 132.6, 132.0, 130.6, 130.4, 130.3, 130.0, 128.5, 128.2, 128.1, 128.0, 127.8, 127.7, 127.2, 127.1, 126.8, 118.6, 113.9, 113.0, 112.3, 110.5, 104.6, 93.4, 82.4, 75.4, 52.3, 51.5, 39.5, 18.7, 11.4 (five signals coincident or not observed). ESI MS *m/z* 814.4 ($[M + Na]^+$, 100), 760.3 ($[M – OMe]^+$, 40). ESI HRMS *m/z* calcd. for $C_{51}H_{51}N_5O_2SiNa$ ($[M + Na]^+$) 814.3548, found 814.3537.

Supplementary data

Supplementary data are available with the article through the journal Web site at http://nrcresearchpress.com/doi/suppl/xxxxx.

Acknowledgements. This work has been generously supported by "Solar Technologies go Hybrid" – an initiative of the Bavarian State Ministry for Science, Research and Art, the DFG "Excellence Initiative" supporting the Cluster of Excellence "Engineering of Advanced Materials" (www.eam.uni-erlangen.de), and the Natural Sciences and Engineering Research Council of Canada (NSERC). D.L. thanks NSERC (PGS-D), the Alberta Ingenuity Fund, the University of Alberta, Alberta Heritage, and the Killam Trusts for scholarship support.

References

1 Anthony, J. E. *Chem. Rev.* **2006**, *106*, 5028–5048.

2 Anthony, J. E. *Angew. Chem. Int. Ed.* **2008**, *47*, 452–483.

3 Anthony, J. E.; Facchetti, A.; Heeney, M.; Marder, S. R.; Zhan, X. *Adv. Mater.* **2010** *22*, 3876–3892.

4 Bendikov, M.; Wudl, F.; Perepichka, D. F. *Chem. Rev.* **2004**, *104*, 4891–4946.

5 Lehnherr, D.; Murray, A. H.; McDonald, R.; Ferguson, M. J.; Tykwinski, R. R. *Chem. Eur. J.* **2009**, *15*, 12580–12584.

6 Vets, N.; Smet, M.; Dehaen, W. *Synlett* **2005**, 217–222.

7 (a) Lehnherr, D.; Murray, A. H.; McDonald, R.; Tykwinski, R. R. *Angew. Chem. Int. Ed.* **2010**, *49*, 6190–6194. (b) Lukman, S.; Musser, A. J.; Chen, K.; Athanasopoulos, S.; Yong, C. K.; Zeng, Z.; Ye, Q.; Chi, C.; Hodgkiss, J. M.; Wu, J.; Friend, R. H.; Greenham, N. C. *Adv. Funct. Mater.* **2015**, *25*, 5452–5461.

8 Lehnherr, D.; Tykwinski, R. R. *Aust. J. Chem.* **2011**, *64*, 919–929.

9 (a) Payne, M. A.; Delcamp, J. H.; Parkin, S. R.; Anthony, J. E. *Org. Lett.* **2004**, *6*, 1609–1612. (b) Anthony, J. E.; Gierschner, J.; Landis, C. A.; Parkin, S. R.; Sherman, J. B.; Bakus II, R. C. *Chem. Commun.* **2007**, 4746–4748. (c) Reichwagen, J.; Hopf, H.; Desvergne, J.-P.; Guerzo, A. D.; Bouas-Laurent, H. *Synthesis* **2005**, 3505–3507. (d) Kitamura, C.; Naito, T.; Yoneda, A.; Kobayashi, T.; Naito, H.; Komatsu, T. *Chem. Lett.* **2009**, *38*, 600–601.

10 (a) Takahashi, T.; Kitamura, M.; Shen, B.; Nakajima, K. *J. Am. Chem. Soc.* **2000**, *122*, 12876–12877. (b) Takahashi, T.; Li, S.; Huang, W.; Kong, F.; Nakajima, K.; Shen, B.; Ohe, T.; Kanno, K.-i. *J. Org. Chem.* **2006**, *71*, 7967–7977.

11 (a) Jiang, J.; Kaafarani, B. R.; Neckers, D. C. *J. Org. Chem.* **2006**, *71*, 2155–2158. (b) Bénard, C. P.; Geng, Z.; Heuft, M. A.; VanCrey, K.; Fallis, A. G. *J. Org. Chem.* **2007**, *72*, 7229–7236.

12 Zhao, Y.; Mondal, R.; Neckers, D. C. *J. Org. Chem.* **2008**, *73*, 5506–5513.

13 (a) Stone, M. T.; Anderson, H. L. *J. Org. Chem.* **2007**, *72*, 9776–9778. (b) Lin, C.-H.; Lin, K.-H.; Pal, B.; Tsou, L.-D. *Chem. Commun.* **2009**, 803–805.

14 (a) Chan, S. H.; Lee, H. K.; Wang, Y. M.; Fu, N. Y.; Chen, X. M. Cai; Z. W.; Wong, H. N. C. *Chem. Commun.* **2005**, 66–68. (b) Wang, Y.-M.; Fu, N.-Y.; Chan, S.-H.; Lee, H.-K.; Wong, H. N. C. *Tetrahedron* **2007**, *63*, 8586–8597.

15 Swartz, C. R.; Parkin, S. R.; Bullock, J. E.; Anthony, J. E.; Mayer, A. C.; Malliaras, G. G. *Org. Lett.* **2005**, *7*, 3163–3166. (b) Tang, M. L.; Oh, J. H.; Reichardt, A. D.; Bao, Z. *J. Am. Chem. Soc.* **2009**, *131*, 3733–3740. (c) Tang, M. L.; Reichardt, A. D.; Wei, P.; Bao, Z. *J. Am. Chem. Soc.* **2009**, *131*, 5264–5273.

16 (a) Lim, Y.-F.; Shu, Y.; Parkin, S. R.; Anthony, J. E.; Malliaras, G. G. *J. Mater. Chem.* **2009**, *19*, 3049–3056.

17 (a) Takahashi, T.; Kashima, K.; Li, S.; Nakajima, K.; Kanno, K.-i. *J. Am. Chem. Soc.* **2007**, *129*, 15752–15753.

18 (a) Anthony, J. E.; Brooks, J. S.; Eaton, D. L.; Parkin, S. R. *J. Am. Chem. Soc.* **2001**, *123*, 9482–9483. (b) Anthony, J. E.; Eaton, D. L.; Parkin, S. R. *Org. Lett.* **2002**, *4*, 15–18. (c) Chen, J.; Subramanian, S.; Parkin, S. R.; Siegler, M.; Gallup, K.; Haughn, C.; Martin, D. C.; Anthony, J. E. *J. Mater. Chem.* **2008**, *18*, 1961–1969. (d) Lehnherr, D.; Tykwinski, R. R. *Org. Lett.* **2007**, *9*, 4583–4586.

19 (a) Allen, C. F. H.; Bell, A. *J. Am. Chem. Soc.* **1942**, *64*, 1253–1260. (b) Kaur, I.; Jia, W.; Kopreski, R. P.; Selvarasah, S.; Dokmeci, M. R.; Pramanik, C.; McGruer, N. E.; Miller, G. P. *J. Am. Chem. Soc.* **2008**, *130*, 16274–16286. (c) Kaur, I.; Miller, G. P. *New J. Chem.* **2008**, *32*, 459–463.

20 (a) Maulding, D. R.; Roberts, B. G. *J. Org. Chem.* **1969**, *34*, 1734–1736. (b) Rauhut, M. M.; Roberts, B. G.; Maulding, D. R.; Bergmark, W.; Coleman, R. *J. Org. Chem.* **1975**, *40*, 330–335. (c) Li, Y.; Wu, Y.; Liu, P.; Prostran, Z.; Gardner, S.; Ong, B. S. *Chem. Mater.* **2007**, *19*, 418–423. (d) Lehnherr, D.; Gao, J.; Hegmann, F. A.; Tykwinski, R. R. *Org. Lett.* **2008**, *10*, 4779–4782.

21 Kobayashi, K.; Shimaoka, R.; Kawahata, M.; Yamanaka, M.; Yamaguchi, K. *Org. Lett.* **2006**, *8*, 2385–2388.

22 Yamada, H.; Yamashita, Y.; Kikuchi, M.; Watanabe, H.; Okujima, T.; Uno, H.; Ogawa, T.; Ohara, K.; Ono, N. *Chem. Eur. J.* **2005**, *11*, 6212–6220. (b) Katsuta, S.; Miyagi, D.; Yamada, H.; Okujima, T.; Mori, S.; Nakayama, K.-i.; Uno, H. *Org. Lett.* **2011**, *13*, 1454–1457.

23 Schwaben, J.; Münster, N.; Breuer, T.; Klues, M.; Harms, K.; Witte, G.; Koert, U. *Eur. J. Org. Chem.* **2013**, 1639–1643.

24 (a) Nguyen, M.-H.; Yip, J. H. K. *Organometallics* **2011**, *30*, 6383–6392. (b) Nguyen, M.-H.; Wong, C.-Y.; Yip, J. H. K. *Organometallics* **2013**, *32*, 1620–1629.

25 Miao, Q.; Lefenfeld, M.; Nguyen, T.-Q.; Siegrist, T.; Kloc, C.; Nuckolls, C. *Adv. Mater.* **2005**, *17*, 407–412.

26 (a) Katsuta, S.; Tanaka, K.; Maruya, Y.; Mori, S.; Masuo, S.; Okujima, T.; Uno, H.; Nakayama, K.-i.; Yamada, H. *Chem. Commun.* **2011**, *47*, 10112–10114. (b) Chang, J.; Qu, H.; OOi, Z.-E.; Zhang, J.; Chen, Z.; Wu, J.; Chi, C. *J. Mater. Chem. C* **2013**, *1*, 456–462.

27 (a) Lu, J.; Ho, D. M.; Vogelaar, N. J.; Kraml, C. M.; Pascal Jr., R. A. *J. Am. Chem. Soc.* **2004**, *126*, 11168–11169. (b) Lu, J.; Ho, D. M.; Vogelaar, N. J.; Kraml, C. M.; Bernhard, S.; Byrne, N.; Kim, L. R.; Pascal Jr., R. A. *J. Am. Chem. Soc.* **2006**, *128*, 17043–17050. (c) Duong, H. M.; Bendikov, M.; Steiger, D.; Zhang, Q.; Sonmez, G.; Yamada, J.; Wudl, F. *Org. Lett.* **2003**, *5*, 4433–4436. (d) Payne, M. M.; Odom, S. A.; Parkin, S. R.; Anthony, J. E. *Org. Lett.* **2004**, *6*, 3325–3328. (e) Tang, M. L.; Mannsfeld, S. C. B.; Sun, Y.-S.; Becerril, H. A.; Bao, Z. *J. Am. Chem. Soc.* **2009**, *131*, 882–883.

28 (a) Bunz, U. H. F.; Engelhart, J. U. *Chem. Eur. J.* **2016**, *22*, 4680–4689. (b) Bunz, U. H. F. *Chem. Eur. J.* **2009**, *15*, 6780–6789. (c) Miao, Q. *Synlett* **2012**, 326–336.

29 (a) Zhang, J.; Pawle, R. H.; Haas, T. E.; Thomas, S. W. *Chem. Eur. J.* **2014**, *20*, 5880–5884. (b) Zhang, J.; Smith, Z. C.; Thomas, S. W. *J. Org. Chem.* **2014**, *79*, 10081–10093. (c) Lehnherr, D.; Tykwinski, R. R. *Materials* **2010**, *3*, 2772–2800.

30 Lehnherr, D.; McDonald, R.; Tykwinski, R. R. *Org. Lett.* **2008**, *10*, 4163–4166.

31 Other donor/acceptor pentacenes, see for example: (a) Tönshoff, C.; Bettinger, H. F.; *Chem. Eur. J.* **2012**, *18*, 1789–1799. (b) Qu, H.; Cui, W.; Li, J.; Shao, J.; Chi, C. *Org. Lett.* **2011**, *13*, 924–927. (c) Schwaben, J.; Münster, N.; Klues, M.; Breuer, T.; Hofmann, P.; Harms, K.; Witte, G.; Koert, U. *Chem. Eur. J.* **2015**, *21*, 13758–13771. (d) Savu, S.-A.; Abb, S.; Schundelmeier, S.; Saathoff, J. D.; Stevenson, J. M.; Tönshoff, C.; Bettinger, H. F.; Clancy, P.; Casu, M. B.; Chassé, T. *Nano Res.* **2013**, *6*, 449–459.

32 Direct attachment of a nitro group at the 1- and 2-positions has been reported, see: Shu, Y.; Lim, Y.-F.; Li, Z.; Purushothaman, B.; Hallani, R.; Kim, J. E.; Parkin, S. R.; Malliaras, G. G.; Anthony, J. E. *Chem. Sci.* **2011**, *2*, 363–368.

33 (a) Zirzlmeier, J.; Lehnherr, D.; Coto, P. B.; Chernick, E. T.; Casillas, R.; Basel, B.; Thoss, M.; Tykwinski, R. R.; Guldi, D. M. *Proc. Natl. Acad. Sci. U.S.A.* **2015**, *112*, 5325–5330. (b) Zirzlmeier, J.; Casillas, R.; Reddy, S. R.; Coto, P. B.; Lehnherr, D.; Chernick, E. T.; Papadopoulos, I.; Thoss, M.; Tykwinski, R. R.; Guldi, D. M. *Nanoscale* **2016**, 8, 10113–10123.

34 (a) Waterloo, A. R.; Kunakom, S.; Hampel, F.; Tykwinski, R. R. *Macromol. Chem. Phys.* **2012**, *213*, 1020–1032. (b) Waterloo, A. R.; Lippert, R.; Jux, N.; Tykwinski, R. R. *J. Coord. Chem.* **2015**, *68*, 3088–3098.

35 (a) Strinitz, F.; Waterloo, A. R.; Tucher, J.; Hübner, E.; Tykwinski, R. R.; Burzlaff, N. *Eur. J. Inorg. Chem.* **2013**, 5181–5186. (b) Strinitz, F.; Tucher, J.; Januszewski, J. A.; Waterloo, A. R.; Stegner, P.; Förtsch, S.; Hüber, E.; Tykwinski, R. R.; Burzlaff, N. *Organometallics*, **2014**, *33*, 5129–5144.

36 Aryl nitro groups are known to be reduced when exposed to $SnCl_2 \cdot xH_2O$ (x = 0 or 2) with or without acid present, see: (a) Xing, W.-K.; Ogata, Y. *J. Org. Chem.* **1982**, *47*, 3577–3581. (b) Bellamy, F. D.; Ou, K. *Tetrahedron Lett.* **1984**, *25*, 839–842.

37 (a) Clark, J. H.; Smith, D. K. *Tetrahedron Lett.* **1985**, *26*, 2233–2236. (b) Kuduk, S. D.; DiPardo, R. M.; Bock, M. G. *Org. Lett.* **2005**, *7*, 577–579.

38 See the Supporting Information for UV–vis absorption spectra of the pentacenes presented herein.

39 See the Supporting Information for details.

40 The wavelength used as the absorption edge for determining E_g^{opt} corresponds to the lowest energy absorption wavelength that has a molar absorptivity (□) ≥ 1000 $L \cdot mol^{-1} \cdot cm^{-1}$.

41 Potential values (E) were calculated using the following equation (except where otherwise noted): $E = (E_{pc} + E_{pa})/2$, where E_{pc} and E_{pa} correspond to the cathodic and anodic peak potentials, respectively. All potentials represent a one-electron reduction or oxidation event. $E_g^{electro}$ determined from the separation between the first oxidation and first reduction potentials.

42 Interplanar distances were calculated from the distance between the least squares planes generated from the carbon atoms of the pentacenes moieties.

43 (a) Takahashi, O.; Kohno, Y.; Iwasaki, S.; Saito, K.; Iwaoka, M.; Tomoda, S.; Umezawa, Y.; Tsuboyama, S.; Nishio, M. *Bull. Chem. Soc. Jpn.* **2001**, *74*, 2421–2430. (b) Nishio, M.; Umezawa, Y.; Honda, K.; Tsuboyama, S.; Suezawa, H. *CrystEngComm* **2009**, *11*, 1757–1788. (c) Kozmon, S.; Matuška, R.; Spiwok, V.; Koča, J. *Chem. Eur. J.* **2011**, *17*, 5680–5690. (d) Takahashi, O.; Kohno, Y.; Nishio, M. *Chem. Rev.* **2010**, *110*, 6049–6076.

44 (a) Zade, S. S.; Zamoshchik, N.; Reddy, A. R.; Fridman-Marueli, G.; Sheberla, D.; Bendikov, M. *J. Am. Chem. Soc.* **2011**, *133*, 10803–10816. (b) Zade, S. S.; M. Bendikov, M. *J. Phys. Org. Chem.* **2012**, *25*, 452–461. (c) Reddy, A. R.; Bendikov, M. *Chem. Commun.* **2006**, 1179–1181. (d) Maliakal, A.; Raghavachari, K.; Katz, H.; Chandross, E.; Siegrist T. *Chem. Mater.* **2004**, *16*, 4980–4986. (d) Miller, G. P.; Mack, J. *Org. Lett.* **2000**, *2*, 3979–3982. (e) Purushothaman, B.; Parkin, S. R. Anthony, J. E. *Org. Lett.* **2010**, *12*, 2060–2063. (f) Coppo, P.; Yeates, S. G. *Adv. Mater.* **2005**, *17*, 3001–3005. (g) Perepichka, D. F. Bendikov, M.; Meng, H.; Wudl, F. *J. Am. Chem. Soc.* **2003**, *125*, 10190–10191. (h) Zhao, D.; Swager, T. M. *Org. Lett.* **2005**, *7*, 4357–4360. (i) Pal, B.; Lin, B.-C.; dela Cerna, M. V. C.; Hsu, C.-P.; Lin, C.-H. *J. Org. Chem.* **2016**, *81*, 6223–6234. (j) Jia, Z.; Li, S.; Nakajima, K.; Kanno, K.-i.; Takahashi, T. *J. Org. Chem.* **2011**, *76*, 293–296. (k) Cao, Y.; Liang, Y.; Zhang, L.; Osuna, S.; Hoyt, A.-L. M.; Briseno, A. L.; Houk, K. N. *J. Am. Chem. Soc.* **2014**, *136*, 10743–10751. (l) Wise, K. E.; Wheeler, R. A. *J. Phys. Chem. A* **1999**, *103*, 8279–8287 (m) Garcia-Borràs, M.; Konishi, A.; Waterloo, A.; Liang, Y.; Cao, Y.; Hetzer, C.; Lehnherr, D.; Hampel, F.; Houk, K. N.; Tykwinski, R. R. *Chem. Eur. J.* **2016**, DOI: 10.1002/chem.201604099.

45 (a) Kivala, M.; Diederich, F. *Acc. Chem. Res.* **2009**, *42*, 235–248. (b) Kato, S.-i.; Diederich, F. *Chem. Commun.* **2010**, *46*, 1994–2006. (c) Michinobu, T.; Boudon, C.; Gisselbrecht, J.-P.; Seiler, P.; Frank, B.; Moonen, N. N. P.; Gross, M.; Diederich, F. *Chem. Eur. J.* **2006**, *12*, 1889–1905.

46 For related reactions, see: (a) Ref 2. (b) Li, S.; Jia, Z.; Nakjima, K.; Kanno, K.-i.; Takahashi, T. *J. Org. Chem.* **2011**, *76*, 9983–9987. (c) Johns, V. K.; Shi, Z.; Hu, W.; Johns, J. B.; Zou, S.; Liao, Y. *Eur. J. Org. Chem.* **2012**, 2707–2710.

47 Gaussian 09, Frisch, M. J.; Trucks, G. W.; Schlegel, H. B.; Scuseria, G. E.; Robb, M. A.; Cheeseman, J. R.; Scalmani, G.; Barone, V.; Mennucci, B.; Petersson, G. A.; Nakatsuji, H.; Caricato, M.; Li, X.; Hratchian, H. P.; Izmaylov, A. F.; Bloino, J.; Zheng, G.; Sonnenberg, J. L.; Hada, M.; Ehara, M.; Toyota, K.; Fukuda, R.; Hasegawa, J.; Ishida, M.; Nakajima, T.; Honda, Y.; Kitao, O.; Nakai, H.; Vreven, T.; Montgomery, J. A., Jr.; Peralta, J. E.; Ogliaro, F.; Bearpark, M.; Heyd, J. J.; Brothers, E.; Kudin, K. N.; Staroverov, V. N.; Kobayashi, R.; Normand, J.; Raghavachari, K.; Rendell, A.; Burant, J. C.; Iyengar, S. S.;

Tomasi, J.; Cossi, M.; Rega, N.; Millam, J. M.; Klene, M.; Knox, J. E.; Cross, J. B.; Bakken, V.; Adamo, C.; Jaramillo, J.; Gomperts, R.; Stratmann, R. E.; Yazyev, O.; Austin, A. J.; Cammi, R.; Pomelli, C.; Ochterski, J. W.; Martin, R. L.; Morokuma, K.; Zakrzewski, V. G.; Voth, G. A.; Salvador, P.; Dannenberg, J. J.; Dapprich, S.; Daniels, A. D.; Farkas, Ö.; Foresman, J. B.; Ortiz, J. V.; Cioslowski, J.; Fox, D. J. Gaussian, Inc., Wallingford CT, 2009.

48 (a) Jarowski, P. D.; Wu, Y.-L.; Boudon, C.; Gisselbrecht, J.-P.; Gross, M.; Schweizer, W. B.; Diederich, F. *Org. Biomol. Chem.* **2009**, *7*, 1312–1322. (b) Wu, Y.-L.; Jarowski, P. D.; Schweizer, W. B.; Diederich, F. *Chem. Eur. J.* **2010**, *16*, 202–211.

49 (a) Busby, E.; Xia, J.; Wu, Q.; Low, J. Z.; Song, R.; Miller, J. R.; Zhu, X.-Y.; Campos, L. M.; Sfeir, M. Y. *Nat. Mater.* **2015**, *14*, 426–433. (b) Also see reference 33.

50 OLEX2: Dolomanov, O.V.; Bourhis, L.J.; Gildea, R.J.; Howard, J.A.K.; Puschmann, H. *J. Appl. Cryst.* **2009**, *42*, 339–341. The method implemented in OLEX2 is based on that described by van der Sluis, P.; Spek, A. L. *Acta Cryst.* **1990**, *A46* 194–201, upon which the SQUEEZE routine in PLATON is also based.

51 Kosynkin, D. V.; Tour, J. M. *Org. Lett.* **2001**, *3*, 991–992.

52 The synthesis of compound **3b** has been previously reported using alternative synthetic procedures, see for examples: (a) Reade, T. H.; Sim, S. A. *J. Chem. Soc., Trans.* **1924**, *125*, 157–160. (b) Kajigaeshi, S.; Kakinami, T.; Yamasaki, H.; Fujisaki, S.; Okamoto, T. *Bull. Chem. Soc. Jpn.* **1988**, *61*, 600–602. (c) Mitzel, F.; Boudon, C.; Gisselbrecht, J.-P.; Seiler, P.; Gross, M.; Diederich, F. *Helv. Chim. Acta* **2004**, *87*, 1130–1157. (d) Niamnont, N.; Siripornnoppakhun, W.; Rashatasakhon, P.; Sukwattanasinitt, M. *Org. Lett.* **2009**, *11*, 2768–2771.